ACS APPLIED MATERIALS & INTERFACES

Research Article

www.acsami.org

Thermosensitive Ionic Microgels via Surfactant-Free Emulsion Copolymerization and in Situ Quaternization Cross-Linking

Xianjing Zhou,[†] Yuanyuan Zhou,[†] Jingjing Nie,[‡] Zhichao Ji,[§] Junting Xu,[†] Xinghong Zhang,[†] and Binyang Du*[,†]

[†]MOE Key Laboratory of Macromolecular Synthesis and Functionalization, Department of Polymer Science & Engineering, Zhejiang University, Hangzhou 310027, China

[‡]Department of Chemistry, Zhejiang University, Hangzhou 310027, China

[§]Department of Polymer Science and Engineering, College of Chemistry, Chemical Engineering and Materials Science, Soochow University, Suzhou 215123, China

Supporting Information

ABSTRACT: A type of thermosensitive ionic microgel was successfully prepared via the simultaneous quaternized cross-linking reaction during the surfactant-free emulsion copolymerization of *N*-isopropylacrylamide (NIPAm) as the main monomer and 1-vinylimidazole or 4-vinylpyridine as the comonomer. 1,4-Dibromobutane and 1,6-dibromohexane were used as the halogenated compounds to quaternize the tertiary amine in the comonomer, leading to the formation of a cross-linking network and thermosensitive ionic microgels. The sizes, morphologies, and properties of the obtained ionic microgels were systematically investigated by using transmission electron microscopy (TEM), dynamic and static light scattering (DLS and SLS), electrophoretic light scattering (ELS), thermogravimetric analyses (TGA), and UV−visible spectroscopy. The obtained ionic microgels were spherical in shape with narrow size distribution. These ionic microgels exhibited thermosensitive behavior and a unique feature of poly(ionic liquid) in aqueous solutions, of which the counteranions of the microgels could be changed by anion exchange reaction with BF_4K or lithium trifluoromethyl sulfonate (PFM-Li). After the anion exchange reaction, the ionic microgels were stable in aqueous solution and could be well dispersed in the solvents with different polarities, depending on the type of counteranion. The sizes and thermosensitive behavior of the ionic microgels could be well tuned by controlling the quaternization extent, the type of comonomer, halogenated compounds, and counteranions. The ionic microgels showed superior swelling properties in aqueous solution. Furthermore, these ionic microgels also showed capabilities to encapsulate and release the anionic dyes, like methyl orange, in aqueous solutions.

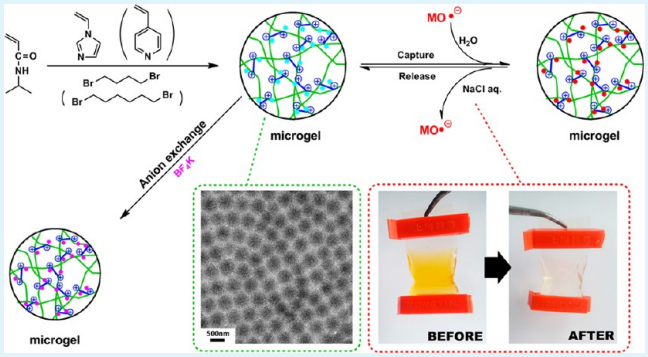

KEYWORDS: *microgels, quaternization cross-linking, ionic, thermosensitive, anion exchange, encapsulation and release*

1. INTRODUCTION

Ionic liquids (ILs), which are organic salts having low melting temperature, such as ethylammonium nitrate, tetraalkylammonium chlorocuprate, and tetra-*n*-hexylammonium benzoate, have attracted significant research interest.[1−3] These ionic liquids have the ability to dissolve a wide range of organic and ionic compounds. Many efforts have been directed at the usage of ionic liquids as green solvents for various polymerization systems.[4] In the past few years, ILs have also been used as monomers to synthesize polymeric ionic liquids (PILs), which are described as a novel class of materials combining the properties of ILs and the specificities of polymers.[5−7] The reported typical PILs were polymers with cations such as imidazolium, pyrrolidonium, and pyridinium and anions such as tetrafluoroborate, hexafluorophosphate, and triflates.[8] In analogy to the case of ILs, PILs can be applied in many different technological fields, such as polymer electrolytes for electrochemical devices,[9−13] materials science,[14,15] analytical chemistry,[16] biotechnology,[17] catalysts,[18,19] and surface science.[20,21] The most notable feature of PILs is the strong influence of the nature of the counteranion on their solubility. This is particularly evident in the case of cationic PILs with different counteranions and their solubility in different solvents. There are two general approaches for fabricating PILs.[8,22,23] One approach was pioneered by Ohno et al.[22] A variety of IL monomers were first synthesized by anion exchange reaction of a cationic 1-vinyl-3-alkyl imidazolium halide-type monomer with different counteranions, and the PILs were then prepared

Received: January 14, 2014
Accepted: March 3, 2014
Published: March 3, 2014

Scheme 1. Synthesis of Thermosensitive Ionic Microgels via Quaternized Cross-Linking Reaction and Their Properties of Anion Exchange and Encapsulation/Release of Anionic Dyes in Water

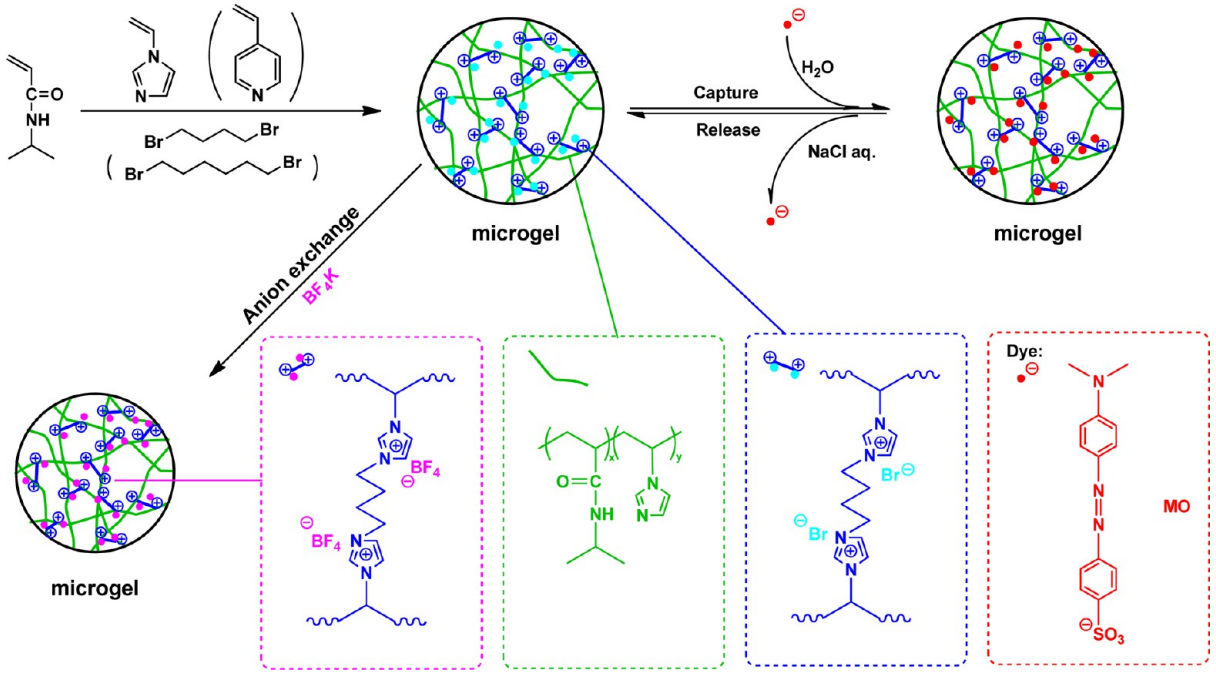

by the direct polymerization of each different IL monomer. The other approach was to first polymerize the imidazolium monomer and then carry out the anion exchange reaction after the polymerization.[8] Because of their characteristic change in physicochemical properties such as solubility, hydrophilicity, or volume change induced by the anion exchange reaction, PILs have been applied to the design of new ion-sensitive smart materials, such as the hydrophilic/hydrophobic switchable surfaces based on PIL polymer brushes,[24,25] ion-sensitive micelles,[26,27] optical sensors based on photonic crystals,[28,29] and reversible porous polymers.[30] For example, Yuan et al.[25] reported the synthesis of poly(ionic liquid) (PIL) nanoparticles grafted with a poly(*N*-isopropylacrylamide) (PNIPAm) brush shell, which showed responsiveness to changes of temperature and ionic strength in aqueous solution. The assembly properties, thermal phase behavior, and microdynamics of poly(*N*-isopropylacrylamide)-*b*-poly(1-butyl-3-vinylimidazolium bromide) [poly(NIPAM-*b*-BVImBr)] micelles in aqueous solution were investigated by combined techniques of dynamic light scattering (DLS), turbidity measurements, and FTIR spectroscopy.[27]

Microgels[29−55] are three-dimensional cross-linked polymeric colloidal particles. Early in 1986, Pelton and Chibante[31] first reported the preparation of monodispersed PNIPAm microgels by surfactant-free emulsion polymerization (SFEP) at elevated temperature (>55 °C). PNIPAm is a thermosensitive polymer in aqueous solution, which exhibits a low critical solution temperature (LCST) at ∼32 °C.[56] As a result, PNIPAm is hydrophilic and soluble in aqueous solution at temperature below its LCST and becomes hydrophobic and insoluble and forms aggregates in aqueous solution above its LCST. By choosing suitable monomers and comonomers, the obtained microgels could respond to various external stimuli, namely, changes in temperature, pH, ionic strength, or others.[32] Because of the unique properties of microgels, numerous investigations have been focused not only on the preparation and physical properties of various microgel systems and the development of new methods for microgel fabrication but also on the exploration of their potential applications as controlled-release systems, in catalysis, in separation technology, as nanoreators, as enzyme immobilization biosensors, and as surface coatings, etc.[33,42,57−60]

Among the responsive microgels reported in the literature, the microgels, which have ionic liquid moieties in the cross-linking network, are scarcely explored. Such ionic microgels may possess the characteristics of PILs besides the general properties of microgels. The synergetic properties of PILs and microgels might render them new functionalities and hence broaden their application potentials. However, there were only a few reports about the preparation of gels or microgels involving ILs or PILs. Winterton et al.[61] reported the synthesis of cross-linked polymer−ionic liquid composite materials by in situ polymerization of vinyl monomers with divinylbenzene (DVB) as the cross-linking agent in ionic liquids (ILs). The obtained composite materials could be suitable for evaluation in catalytic membranes.[61] Muldoon and Gordon[18] reported the gel-type polymer beads made entirely from the IL monomer, 1-butyl-3-vinylimidazolium bis(trifluoromethylsulfonyl)imide ([bvim][Tf_2N]), by the suspension polymerization with a dicationic salt, 1,8-di(vinylimidazolium)-octane bis-[(trifluoromethyl)sulfonyl] amide ([C_8(vim)$_2$][Tf_2N]), as the cross-linker. The obtained polymer beads could swell in ketones, short-chain alcohols, and polar aprotic solvents.[18] They also demonstrated that such polymer beads could have potential applications as catalyst support.[18] Mecerreyes et al.[17] reported a new type of PIL microgel prepared by the concentrated emulsion polymerization of the ionic liquid monomer, 1-vinyl-3-ethylimidazolium bromide (ViEtIm$^+$Br$^-$), with *N*,*N*-dimethylenebisacrylamide (BIS) as the cross-linking agent. However, the concentrated emulsion polymerization led to the microgels with a large size and a broad size distribution ranging from 0.5 to 20 μm.[17] The obtained microgels having a

dx.doi.org/10.1021/am500291n | ACS Appl. Mater. Interfaces 2014, 6, 4498−4513

Table 1. Preparation Conditions and Results of Thermosensitive Ionic Microgels

sample codes	NIPAm (mmol)	comonomer VIM (mmol)	cross-linking agent (mmol) 4VP (mmol)	1,4-dibromobutane	1,6-dibromohexane	SLS R_g[a] (nm)	DLS R_h[a] (nm)	PDI[b]	R_g/R_h	TEM D (nm)	swelling ratio (V_{25}/V_{60})
PNI4-1#	2	0.2		0.1		269	344	0.04	0.78	436 ± 33	37
PNI4-2#		0.3		0.075		246	471	0.16	0.52	579 ± 23	468
PNI4-3#		0.3		0.1		244	382	0.25	0.64	491 ± 28	137
PNI4-4#		0.3		0.15		230	307	0.13	0.75	413 ± 23	9
PNI4-5#		0.4		0.1		284	459	0.08	0.62	541 ± 36	247
PNI4-6#		0.3		0.3		/	180	0.01	/	320 ± 16	7
PNI6-1#		0.2			0.1	239	270	0.14	0.89	420 ± 17	57
PNI6-2#		0.3			0.075	264	461	0.09	0.57	481 ± 36	816
PNI6-3#		0.3			0.1	218	383	0.12	0.57	517 ± 22	380
PNI6-4#		0.3			0.15	170	211	0.18	0.81	347 ± 21	186
PNI6-5#		0.4			0.1	265	460	0.21	0.58	408 ± 28	3490
PNI6-6#		0.3			0.3	/	188	0.10	/	388 ± 20	176
PNP4-1#			0.2	0.1		179	241	0.12	0.74	458 ± 21	26
PNP4-2#			0.3	0.075		139	202	0.01	0.69	338 ± 14	10
PNP4-3#			0.3	0.1		103	175	0.05	0.59	253 ± 12	8
PNP4-4#			0.3	0.15		92	164	0.11	0.56	207 ± 9	6
PNP4-5#			0.4	0.1		83	162	0.14	0.51	201 ± 15	5
PNP4-6#			0.3	0.3		/	124	0.18	/	217 ± 13	5

[a]Measured at 25 °C. [b]PDI = polydispersity index of the thermosensitive ionic microgels measured by DLS.

bromide anion could be dispersed in water and methanol (MeOH). After anion exchange reaction, the microgels bearing hydrophobic counterions such as $CF_3SO_3^-$, $(CF_3SO_3)_2N^-$, and $(CF_3CF_2SO_2)_2N^-$ could swell in nonpolar solvents such as acetone and tetrahydrofuran (THF). Furthermore, the microgels showed a larger size after anion exchange than the precursor microgels with a bromide anion.[17] Such PIL microgels showed good thermal stability and could be used as glucose biosensors.[17] Xiong et al.[62−64] reported the synthesis of cross-linked polymeric nanoparticles (CLPNs) by radical copolymerization of monomers of ILs such as 4-vinylbenzyltriphenylphosphorous chloride and 4-vinylbenzyl-tributylphosphorous chloride and the cross-linking agents of ethylene glycol dimethacrylate (EGDMA), DVB, or 1,4-butanediyl-3,3′-bis-1-vinylimidazolium halides in selective solvents. The obtained CLPNs had the mean diameter range of 10−100 nm with a broad size distribution.[62−64]

In the present work, a one-pot route was reported to synthesize a new type of thermosensitive ionic microgel with a narrow size distribution and unique feature of PILs. *N*-Isopropylacrylamide was used as the main monomer to offer the resultant microgel's thermosensitive character. 1-Vinylimidazole (VIM) or 4-vinylpyridine (4VP) was chosen as the comonomer. Such comonomers had tertiary amines, which could be quaternized by the halogenated compounds. 1,4-Dibromobutane and 1,6-dibromohexane were then used as the halogenated compounds to quaternize the tertiary amines in the comonomers, leading to the formation of the cross-linking network and thermosensitive ionic microgels with ionic liquid moieties, as illustrated in Scheme 1. Three series of thermosensitive ionic microgels, p(*N*-isopropylacrylamide-*co*-1-vinylimidazole)/1,6-dibromohexane microgels [P(NIPAm-*co*-VIM)/1,6-dibromohexane, PNI6], p(*N*-isopropylacrylamide-*co*-1-vinylimidazole)/1,4-dibromobutane microgels [P(NIPAm-*co*-VIM)/1,4-dibromobutane, PNI4], and p(*N*-isopropylacrylamide-*co*-4-vinylpyridine)/1,4-dibromobutane microgels [P(NIPAm-*co*-4VP)/1,4-dibromobutane, PNP4], were thus obtained. These ionic microgels contained imidazolium or pyridinium moieties with bromide ions as the counterions. The ionic microgels exhibited thermosensitive behavior and the unique feature of poly(ionic liquids) in aqueous solutions, of which the counteranions of the microgels could be changed by an anion exchange reaction with BF_4K or lithium trifluoromethyl sulfonate (PFM-Li). Transmission electron microscopy (TEM), dynamic and static light scattering (DLS and SLS), electrophoretic light scattering (ELS), thermogravimetric analyses (TGA), and UV−visible spectroscopy were employed to systematically investigate the sizes, morphologies, and properties of the obtained ionic microgels. The sizes and thermosensitive behavior of the obtained ionic microgels could be tuned by varying the quaternization extent, comonomers, and halogenated compounds as well as the counteranions.

2. EXPERIMENTAL SECTION

2.1. Chemical and Materials. 4-Vinylpyridine (4VP) and 1,4-dibromobutane were distilled under vacuum before being used. *N*-Isopropylacrylamide (NIPAm), 1-vinylimidazole (VIM), 1,6-dibromohexane, BF_4K, lithium trifluoromethyl sulfonate (PFM-Li), 2,2′-azobis(2-methylpropionamidine) dihydrochloride (AIBA), *α*,*α*′-azodiisobutyronitrile (AIBN), ethanediol bis(2-bromoacetate), potassium peroxodisulfate (KPS), *N*,*N*,*N*′,*N*′-tetramethylethylenediamine (TEMED), $AgNO_3$, ferric ammonium alum ($NH_4Fe(SO_4)_2{\cdot}12H_2O$), NH_4SCN, methyl orange (MO), NaCl, 1,4-dioxane, methanol, acetone, and tetrahydrofuran were used as received without further purification.

2.2. Fabrication of the Thermosensitive Ionic Microgels. The thermosensitive ionic microgels were prepared via the simultaneous quaternized cross-linking reaction during the surfactant-free emulsion copolymerization (SFEP) of *N*-isopropylacrylamide (NIPAm) as the main monomer and 1-vinylimidazole (VIM) or 4-vinylpyridine (4VP) as the comonomer in the presence of 1,4-dibromobutane or 1,6-dibromohexane. Given amounts of NIPAm, VIM (or 4VP), and 1,4-dibromobutane (or 1,6-dibromohexane) were added into 45 mL of deionized water at 70 °C under vigorous stirring. Oxygen was eliminated by bubbling nitrogen through the reaction solution for 20 min. Afterward, 5 mL of AIBA aqueous solution (5 mg/mL) was added into the solution to initiate the polymerization. The reaction was then kept at 70 °C for 6 h. The resultant microgels were purified

Table 2. Feed Compositions and Results of the P(NIPAm-*co*-VIM)/1,6-Dibromohexane Microgels before and after Anion Exchange Reaction

					DLS			TEM
sample code	microgels	salts	feed ratio[a]	SLS R_g (nm)[b]	R_h (nm)[b]	PDI[c]	R_g/R_h	D (nm)
PNI6-2#	PNI6-2#	/	/	264	461	0.09	0.57	481 ± 36
PNI6-2#−BF_4-1	PNI6-2#	BF_4K	2:1	258	438	0.01	0.59	606 ± 26
PNI6-2#−BF_4-2			2:2	280	421	0.09	0.67	609 ± 25
PNI6-2#−BF_4-3			2:3	252	358	0.05	0.70	607 ± 18
PNI6−2#- PFM-1		PFM-Li	2:1	255	440	0.04	0.58	539 ± 15
PNI6-2#− PFM-2			2:2	254	419	0.05	0.61	587 ± 33
PNI6-2#− PFM-3			2:3	239	393	0.20	0.61	706 ± 23
PNI6-4#−BF_4	PNI6-4#	BF_4K	2:3	/	/	/	/	/
PNI6-4#−PFM		PFM-Li	2:3	/	/	/	/	/

[a]Molar ratio of quaternized imidazole moieties in microgels to the salts added. [b]Measured at 25 °C. [c]PDI = polydispersity index of the ionic microgels measured by DLS.

by dialysis against deionized water with a molecular-weight-cutoff (MWCO) of 14 000 dialysis tube for 3 days. Three series of microgels were prepared with fixed NIPAm concentration and various comonomers and halogenated compounds, as listed in Table 1. P(*N*-isopropylacrylamide-*co*-1-vinylimidazole)/1,6-dibromohexane microgels [P(NIPAm-*co*-VIM)/1,6-dibromohexane], P(*N*-isopropylacrylamide-*co*-1-vinylimidazole)/1,4-dibromobutane microgels [P(NIPAm-*co*-VIM)/1,4-dibromobutane], and P(*N*-isopropylacrylamide-*co*-4-vinylpyridine)/1,4-dibromobutane microgels [P(NIPAm-*co*-4VP)/1,4-dibromobutane] were coded as PNI6, PNI4, and PNP4, respectively.

To check the formation mechanism of the obtained ionic microgels, the variations of the hydrodynamic size and size distribution of microgels with sample code of PNI4-4# were monitored by DLS via direct sampling of product at different polymerization times.

To further study the formation mechanism of the ionic microgels, the fabrication of microgels was also attempted at room temperature. NIPAm (0.2264 g), VIM (27 μL), 1,6-dibromohexane (23 μL), and KPS (0.01 g) were added into 45 mL of deionized water at 25 °C under vigorous stirring. Oxygen was eliminated by bubbling nitrogen through the reaction solution for 20 min. Afterward, 5 mL of TEMED aqueous solution (2 μL/mL) was added into the solution to initiate the polymerization. The reaction was then kept at 25 °C for 4 days. The feed ratio was the same as that of PNI6-4# microgels. The variation of the hydrodynamic size and size distribution of samples were again monitored by dynamic light scattering (DLS) via direct sampling of product at different polymerization times. The resultant samples were purified by dialysis against deionized water with a molecular-weight-cutoff (MWCO) of 3500 dialysis tube for 3 days and then subjected to freeze-drying.

2.3. Synthesis of Linear Copolymer. The linear copolymer of poly(*N*-isopropylacrylamide-*co*-1-vinylimidazole) [P(NIPAm-*co*-VIM)] was synthesized by free radical copolymerization of NIPAm and VIM. Briefly, NIPAm (1.5 g) and VIM (0.18 mL) were first dissolved in 1,4-dioxane (18 mL) in a three-neck flask with a magnetic stir bar. AIBN (0.036 g) was then dissolved in this mixture. Afterward, the mixture was degassed by bubbling with nitrogen for 20 min and then placed in an oil bath with preset temperature at 70 °C. The polymerization was allowed to proceed for 24 h. The reaction was then stopped, and the mixture was concentrated with a rotary evaporator until the solution volume was reduced to be approximately 1/4 of the initial volume. The resultant copolymer was then precipitated into cold diethyl ether. The precipitate was dissolved in ethanol and again precipitated by cold diethyl ether. The dissolution and precipitation processes were repeated several times to remove impurities. The final purified copolymers were dried in a vacuum at 30 °C and then stored in a desiccator for further use. The linear copolymer of poly(*N*-isopropylacrylamide-*co*-4-vinylpyridine) [P(NIPAm-*co*-4VP)] was prepared in the same manner.

2.4. Determination of the Degree of Quaternization Reaction. The degree of quaternization reaction of the obtained ionic microgels could be determined by measuring the concentration of bromide ions in the microgel suspensions. Bromide ions were determined by Volhard's method with the following analytical procedure: (1) Freeze-dried microgels with sample codes of PNI6-2#, PNI6-3#, and PNI6-4# were first swollen well in 10 mL of deionized water, respectively. (2) An amount of 2 mL of $AgNO_3$ with concentration of 0.045 mol/L was added into the microgel suspensions and homogenized, which were allowed to rest in the dark for 1 day to flocculate AgBr completely. (3) The excess Ag^+ was obtained by several centrifugations and redispersions in deionized water cycles. The supernatant of each cycle was gathered together. (4) An amount of 2 mL of 20% ferric ammonium alum was added into the supernatant as the indicator, and the supernatant was then titrated with the standard solution of NH_4SCN with a concentration of 0.01 mol/L until a permanent reddish brown color was obtained.

2.5. Anion Exchange Reaction of the Ionic Microgels. The obtained thermosensitive ionic microgels with sample codes of PNI4-2#, PNI6-2#, and PNI6-4# were chosen to investigate the effect of counteranions on the properties of the microgels. Various amounts of salts, i.e., BF_4K and PFM-Li, were added into the suspension of microgels in deionized water with vigorous stirring for the anion exchange reaction, respectively. The reaction lasted for 24 h at room temperature. The resultant microgels with various types or amounts of counteranion were purified by several centrifugation and redispersion processes with the supernatant replaced by deionized water. The feed compositions of anion exchange reaction with PNI6-2# and PNI6-4# microgels were given in Table 2. The experimental conditions of PNI4-2# microgels were similar to those of PNI6 microgels.

2.6. Encapsulation and Release of Dye in Aqueous Solution. The obtained thermosensitive ionic microgels with sample code of PNI4-2#, PNI4-3#, and PNI4-4# were chosen to test the encapsulation and release capabilities of dye in aqueous solution. Methyl orange (MO) was used as the model dye. Typically, 10 mg of thermosensitive ionic microgels and various amounts of MO (5.1, 3.4, 1.7, and 1.0 mg, respectively) were mixed and stirred in 5 mL of deionized water for 2 h. The mixture was then transferred into a dialysis tube with MWCO of 3500 and dialyzed in deionized water for 1 week. The deionized water was changed every 3 h for the first day and every 12 h for the rest of the days. After dialysis, the ionic microgels with encapsulation of MO were then subjected to freeze-drying. The resulting dried microgels loaded with MO were redissolved in water to give a concentration of 0.05 mg/mL and then analyzed by UV−vis spectroscopy. The absorption intensity at 460 nm was used to calculate the amounts of MO encapsulated within the ionic microgels. Note that MO exhibits an UV absorption peak at 460 nm.

Release of MO from the thermosensitive ionic microgels was investigated by dialyzing the aqueous dispersions of MO-encapsulated microgels in 0.1 M NaCl aqueous solutions. Typically, 5 mL aqueous dispersions of MO-encapsulated microgels with a concentration of 1 mg/mL were added into a dialysis tube with MWCO of 3500, which

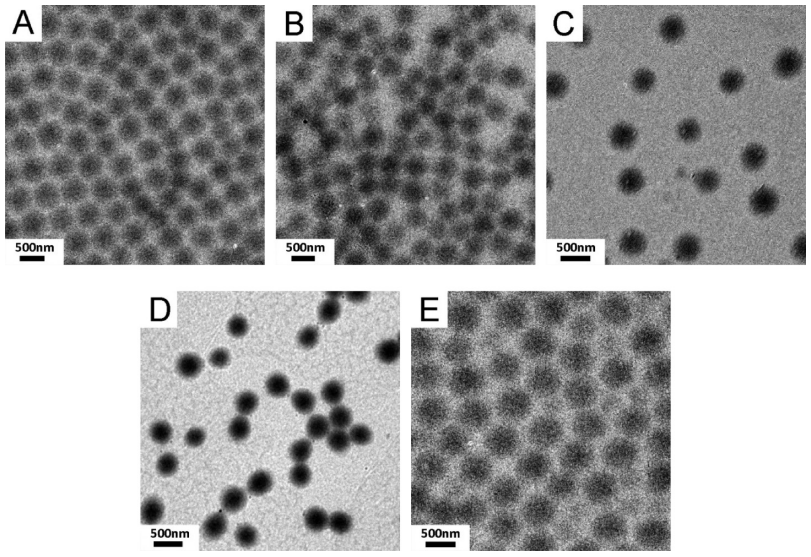

Figure 1. Representative TEM images of the PNI4 series of thermosensitive ionic microgels, i.e., P(NIPAm-*co*-VIM)/1,4-dibromobutane microgels. (A) PNI4-1#, (B) PNI4-2#, (C) PNI4-3#, (D) PNI4-4#, and (E) PNI4-5#.

was then placed into 50 mL of NaCl aqueous solutions (0.1 M). At each time interval, 3 mL of the surrounding medium was sampled and replaced with 3 mL of fresh NaCl aqueous solutions (0.1 M). The sampled solutions were measured by UV−vis spectroscopy, and the absorption intensities at 460 nm were used to calculate the amounts of MO released from the microgels.

2.7. Characterization. The hydrodynamic size and size distribution of the obtained thermosensitive ionic microgels were measured by dynamic light scattering (DLS) at a scattering angle θ of 90° as a function of temperatures using a 90 Plus Particle Size Analyzer (Brookhaven Instruments Corp.). The wavelength of laser light λ was 635 nm. For each temperature, the sample solutions were equilibrated for 10−15 min. The zeta potentials ξ of the ionic microgels were also measured by electrophoretic light scattering (ELS) using the same Zeta Plus particle size analyzer. The pH values of sample solutions were measured by a pH meter (FE20, METTLER TOLEDO).

The static light scattering (SLS) of the obtained thermosensitive ionic microgel suspensions was carried out by a commercial spectrometer Brookhaven BI-200SM in the Department of Polymer Science and Engineering, Soochow University. The SLS measurements were performed at 25 °C, and the sample solutions were equilibrated for 15 min. The range of scattering angle θ used for SLS was from 30° to 130° with a step of 5°. The wavelength of laser light λ was 637 nm.

Transmission electron microscopy (TEM) measurements were carried out by a JEOL JEM-1230 electron microscope operated at an acceleration voltage of 60 kV. The TEM samples were prepared by dip coating with Formvar-coated copper grids into the microgel suspensions. The solvent was gently absorbed away by a filter paper. The grids were then allowed to dry in air at room temperature before observation.

Thermogravimetric analyses (TGA) of the thermosensitive ionic microgels before and after anion exchange reaction were performed by using a Perkin-Elmer Pyris 1 instrument from 50 to 800 °C with a heating rate of 10 °C/min under a nitrogen atmosphere. UV−visible spectra were recorded on a Cary 300 instrument (Varian Australia Pty Ltd.). FTIR spectra were recorded on a Vector 22 Bruker spectrometer. ^{1}H NMR spectra were recorded on a 400 MHz Varian Mercury Plus NMR instrument with D_2O as solvent. Weight-average molecular weight (M_w) and polydispersity index (PDI) were determined by gel permeation chromatography (GPC) with *N*,*N*-dimethylformamide (DMF) as eluent and narrow-polydispersity poly(methyl methacrylate) (PMMA) as the calibration standard.

3. RESULTS AND DISCUSSION

3.1. Fabrication of the Thermosensitive Ionic Microgels. The thermosensitive ionic microgels were successfully obtained via the simultaneous quaternized cross-linking reaction during the surfactant-free emulsion copolymerization (SFEP) of *N*-isopropylacrylamide (NIPAm) as the main monomer and 1-vinylimidazole (VIM) or 4-vinylpyridine (4VP) as the comonomer at 70 °C in the presence of 1,4-dibromobutane or 1,6-dibromohexane. The quaternization of the tertiary amine of the comonomer (VIM or 4VP) with dibromo compounds (1,4-dibromobutane or 1,6-dibromohexane) successfully led to the formation of cross-linking networks and thermosensitive ionic microgels. The yields of the products were approximately 73%∼86%. Figure 1 shows the representative TEM images of the resultant PNI4 series of thermosensitive ionic microgels. The obtained thermosensitive ionic microgels were spherical in shape with a narrow size distribution. The average diameters of the thermosensitive ionic microgels calculated from the TEM images were 436 ± 33 nm, 579 ± 23 nm, 491 ± 28 nm, 413 ± 23 nm, and 541 ± 36 nm for the ionic microgels with sample codes of PNI4-1#, PNI4-2#, PNI4-3#, PNI4-4#, and PNI4-5#, respectively. The representative TEM images of PNI6 and PNP4 series of ionic microgels were given as Figures S1 and S2 in the Supporting Information.

The average diameters of the thermosensitive ionic microgels were calculated from the TEM images and summarized in Table 1. It can be seen that when the amounts of comonomer (VIM or 4VP, 0.3 mmol) were fixed the increase of quaternization ratio led to the decrease of sizes for the resultant thermosensitive ionic microgels. In such thermosensitive ionic microgels, the quaternization ratio represented the cross-linking density of the resultant microgel networks. It was understandable that increasing the quaternization ratio led to the higher cross-linking density of the microgel networks and hence the smaller microgel sizes.

FTIR measurements were carried out to confirm the quaternization reaction of 1,4-dibromobutane and 4VP for the PNP4 series of ionic microgels. Figure 2 shows the FTIR spectra of the obtained P(NIPAm-*co*-4VP) (PNP) linear

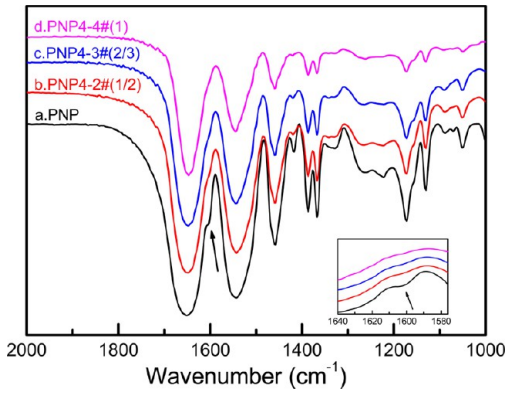

Figure 2. FTIR spectra of the P(NIPAm-*co*-4VP) (PNP) linear polymer (a) and P(NIPAm-*co*-4VP)/1,4-dibromobutane microgels with fixed amount of 4VP (0.3 mmol) and various amounts of 1,4-dibromobutane, i.e., with various quaternization ratios of 1/2 (PNP4-2#, b), 2/3 (PNP4-3#, c), and 1 (PNP4-4#, d). The inset was the FTIR spectra of PNP4 microgels with enlarged X scale.

copolymer and P(NIPAm-*co*-4VP)/1,4-dibromobutane microgels with a fixed amount of 4VP (0.3 mmol) and various amounts of 1,4-dibromobutane, i.e., with various quaternization ratios of 1/2 (PNP4-2#), 2/3 (PNP4-3#), and 1 (PNP4-4#). Note that the quaternization ratio presented the molar ratio of bromo groups in 1,4-dibromobutane or 1,6-dibromohexane to imidazole moieties of VIM or pyridine moieties of 4VP. The characteristic absorption bands at 1652, 1542, and 1458 cm^{-1} could be ascribed to the C═O stretching vibration, N−H stretching vibration, and the methyl group asymmetric bending vibrations of the PNIPAm segments, respectively. The absorption bands at 1600, 1557 cm^{-1} and at 1415, 1221 cm^{-1} could be assigned to the C═C stretching vibrations and C−N stretching vibration of pyridine rings of 4VP segments, respectively (seen in Figure 2a). As reported in the literature,[65] after quaternization reaction, the shift of the absorption band at 1600 cm^{-1} toward higher wavenumber, i.e., 1638 cm^{-1}, was observed for the pyridine ring of 4VP segments.[65] For the P(NIPAm-*co*-4VP)/1,4-dibromobutane microgels, with increasing the quaternization ratio from 0 to 1, the absorption peaks of pyridine rings at 1600 cm^{-1} decreased gradually until they disappeared, which was consistent with the formation of the pyridinium cation.

To determine the exact degree of quaternization reaction, the concentration bromide ions of the obtained microgels were determined by Volhard's method. The microgels with sample codes of PNI6-2#, PNI6-3#, and PNI6-4# were chosen as representatives. The titration procedure was mentioned above in the Experimental Section. Table 3 summarized the results of titration. The degrees of quaternization of PNI6-2#, PNI6-3#, and PNI6-4# microgels were calculated by Volhard's titration to be 45.7%, 63.7%, and 94.0%, respectively. These values suggest that the halogenated compound (1,6-dibromohexane) almost completely reacted with the comonomer VIM within the experimental errors.

^{1}H NMR measurements were also carried out to confirm the degree of quaternization reaction (see Figure S3 in Supporting Information). However, because the obtained ionic microgels could only swell but not dissolve in water, the NMR signals were too weak to distinguish the samples with different quaternization ratios.

The hydrodynamic radius R_h and thermosensitive behavior of the obtained PNI4, PNI6, and PNP4 series of thermosensitive ionic microgels were investigated by dynamic light scattering (DLS). Figure 3 shows the hydrodynamic radius of the PNI6 series of microgels as a function of temperature. The PNI6 series of ionic microgels exhibited thermosensitive behavior (Figure 3) and narrow size distribution (Table 1). The hydrodynamic radius of the PNI6 series of ionic microgels decreased with increasing measuring temperatures. The hydrodynamic radius of PNI6 ionic microgels at a given temperature decreased with increasing quaternization ratio when the amount of VIM was fixed to be 0.3 mmol (Figure 3A). In the case of PNI6 ionic microgels, the quaternization ratio meant the molar ratio of bromo groups of 1,6-dibromohexane to the imidazole moieties of VIM in the P(NIPAm-*co*-VIM)/1,6-dibromohexane microgels. For simplicity, the quaternization ratio here and following was used to refer to the feeding quaternization ratio. Furthermore, the volume phase transition temperature (VPTT) of the PNI6 ionic microgels slightly shifted to the lower temperature, and the temperature range of phase transition became broader with increasing quaternization ratio. The VPTTs of PNI6-2#, PNI6-3#, and PNI6-4# microgels were found to be 45, 43, and 42 °C, respectively (Figure 3A). Similar results were observed for PNI4 and PNP4 series of thermosensitive ionic microgels, i.e., the P(NIPAm-*co*-VIM)/1,4-dibromobutane and P(NIPAm-*co*-4VP)/1,4-dibromobutane microgels (see Supporting Information). As mentioned above, increasing the quaternization ratio meant the increase of cross-linking density of the microgel networks, which usually led to the decrease of microgel sizes and the broadened phase transition.[32,33,43,49]

However, when the amount of 1,6-dibromohexane was fixed (0.1 mmol), increasing the amount of hydrophilic VIM led to the ionic microgels with larger particle sizes and higher VPTT, as shown in Figure 3B. The average hydrodynamic radii of the PNI6 ionic microgels with sample codes of PNI6-1#, PNI6-3#, and PNI6-5# at 25 °C were 270, 383, and 460 nm, respectively.

Table 3. Analyzed Br^- Contents for the Ionic Microgels

						degree of quaternization (%)	
sample code	freeze-dried microgels (mg)	SCN^- (mL)	excess Ag^{+a} (*10^{-5} mol)	$Br_{VO}{}^{-b}$ (*10^{-5} mol)	$Br_{th}{}^{-c}$ (*10^{-5} mol)	VO[d]	theory[d]
PNI6-2#	41.3	7.1	7.1	1.9	2.1	45.7	50.0
PNI6-3#	47.7	6.0	6.0	3.0	3.2	63.7	66.7
PNI6-4#	42.5	5.2	5.2	3.8	4.0	94.0	100.0

[a]The content of excess Ag^+ was calculated by the product of the volume and concentration of NH_4SCN titrant (0.01 mol/L). [b]$Br_{VO}{}^-$: the content of Br^- in microgels by Volhard's titration was calculated by the initial amount of $AgNO_3$ minus the content of excess Ag^+. [c]$Br_{th}{}^-$: the theoretical content of Br^- in microgels was calculated by the feed ratio of freeze-dried microgels. [d]The degree of quaternization calculated by Volhard's titration and the feed quaternization ratio of microgels.

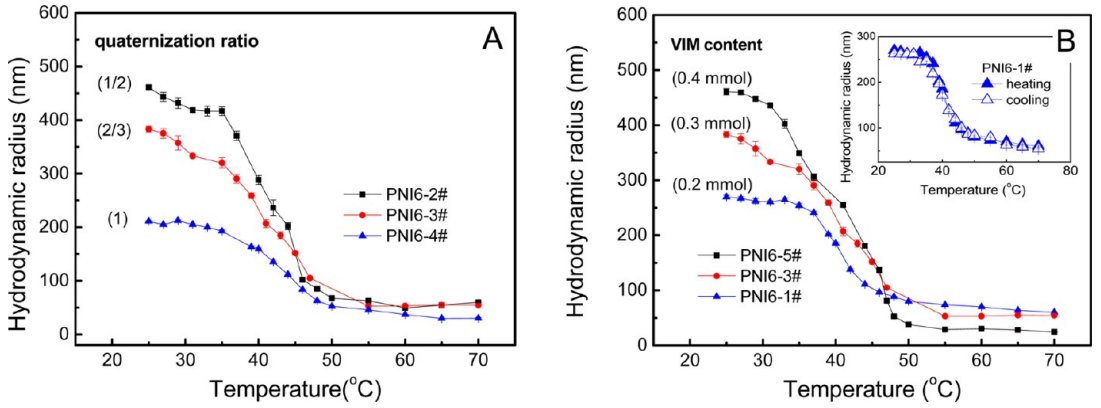

Figure 3. Hydrodynamic radii of the PNI6 series of thermosensitive ionic microgels measured by DLS as a function of measuring temperature (A) with fixed amount of VIM (0.3 mmol) and various amounts of 1,6-dibromohexane, i.e., with various quaternization ratios and (B) with various amounts of VIM and a fixed amount of 1,6-dibromohexane (0.1 mmol). The inset of (B) was the evolution of the hydrodynamic radius of PNI6-1# microgels during the heating and cooling cycles.

The volume phase transition temperatures (VPTTs) of PNI6-1#, PNI6-3#, and PNI6-5# ionic microgels were determined to be 40, 43, and 47 °C, respectively. These results were similar to those reported by Karl-Heinz et al.[66] They obtained the P(NIPAm-*co*-VIM) microgel particles with *N*,*N*′-methylenebisacrylamide as a cross-linking agent in water/oil inverse emulsion used as carriers for enzyme encapsulation. They indicated that the size of the microgels depends on the amount of VIM used as a comonomer in the polymerization process, and the increase of the VIM content in PNIPAm microgels induced higher swelling mainly due to the hydrophilic character of VIM and electrostatic repulsion between partially ionized VIM groups.[66] Furthermore, the thermosensitive behavior of the ionic microgels was reversible, as shown in the inset of Figure 3B. When the temperature was cooled from 70 °C down to room temperature (i.e., 25 °C), the hydrodynamic radius of the PNI6-1# ionic microgels increased again along the similar track of the heating procedure. No hysteresis of hydrodynamic radius in the heating and cooling cycle was observed for PNI6-1# ionic microgels.

Similar thermosensitive behaviors were observed for PNI4 series of thermosensitive ionic microgels, i.e., P(NIPAm-*co*-VIM)/1,4-dibromobutane microgels. With a fixed amount of 1,4-dibromobutane, the increase of amount of hydrophilic VIM led to the PNI4 ionic microgels with larger particle sizes and higher VPTT, as shown in Figure S4 (Supporting Information). However, the opposite results were observed for a PNP4 series of thermosensitive ionic microgels with hydrophobic 4VP as the comonomer. With a fixed amount of 1,4-dibromobutane, the increase of amount of hydrophobic 4VP led to the PNP4 ionic microgels with smaller particle sizes and lower VPTT, as shown in Figure S5 (Supporting Information). Snowden et al.[67] and Vincent et al.[68] also reported that the dependence of temperature on the P(NIPAm-*co*-4VP) microgel particles was affected by the molar ratio of 4VP/NIPAm.[67,68] A continuous decrease in the particle diameter could be observed with increasing concentration of 4VP in the P(NIPAm-*co*-4VP) microgels.[67,68] The hydrodynamic radius R_h measured by DLS and the average diameter calculated from TEM images of the three series of thermosensitive ionic microgels were summarized in Table 1. Both DLS and TEM results indicated that all of the obtained thermosensitive ionic microgels were with narrow size distribution.

The swelling ratios of the PNI6, PNI4, and PNP4 series of thermosensitive ionic microgels were also calculated and listed in Table 1. Note that the volume V_{60} of the thermosensitive ionic microgels at 60 °C was taken as the reference state, and the swelling ratio was given as the ratio of the volume V_{25} of the microgels at 25 °C to the reference volume at 60 °C, i.e., V_{25}/V_{60}. Figure 4 shows the swelling ratio of the three series of thermosensitive ionic microgels as a function of quaternization ratio. It can be clearly observed that with fixed amounts of comonomer the swelling ratios of the three series of microgels decreased with increasing quaternization ratio, that is, the cross-linking density of the microgels, regardless of the types of comonomer (VIM and 4VP) and quaternization cross-linking agent (1,6-dibromohexane and 1,4-dibromobutane). It was reasonable because the increase of quaternization ratio led to the increase of cross-linking density of the microgel networks, which usually resulted in the lower swelling ratio. The highest swelling ratios obtained here could reach ca. 816 and 468 for

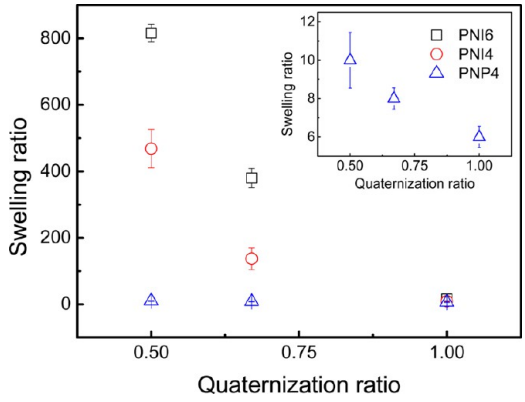

Figure 4. Swelling ratio of the PNI6, PNI4, and PNP4 series of thermosensitive ionic microgels with a fixed amount of comonomer (VIM or 4VP, 0.3 mmol) and various amounts of quaternized cross-linking agent (1,4-dibromobutane or 1,6-dibromohexane), i.e., with various quaternization ratios as measured by DLS. The inset was the swelling ratio of PNP4 microgels with enlarged Y scale. The volume V_{60} of the thermosensitive ionic microgels at 60 °C was taken as the reference state, and the swelling ratio was given as the ratio of the volume V_{25} of the microgels at 25 °C to the reference volume at 60 °C, i.e., V_{25}/V_{60}.

dx.doi.org/10.1021/am500291n | ACS Appl. Mater. Interfaces 2014, 6, 4498−4513

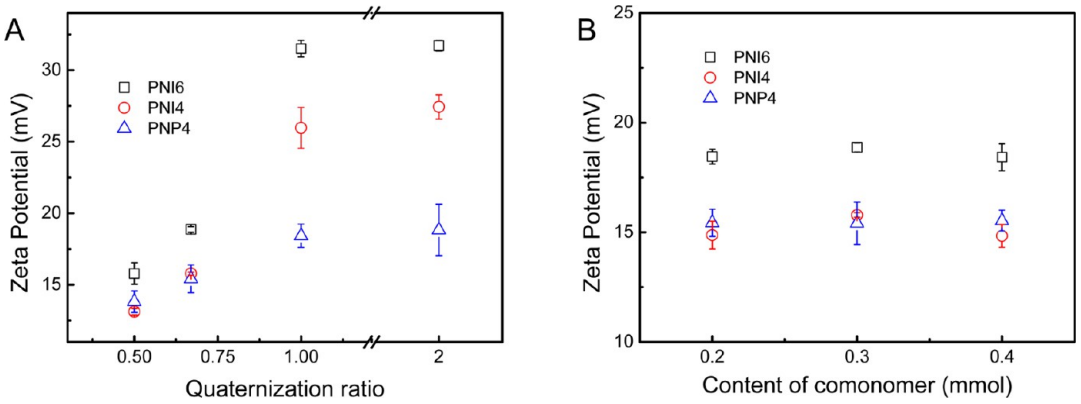

Figure 5. Zeta potentials of the PNI6, PNI4, and PNP4 series of thermosensitive ionic microgels (A) with fixed amounts of comonomer (VIM or 4VP, 0.3 mmol) and various amounts of quaternized cross-linking agent (1,6-dibromohexane or 1,4-dibromobutane), i.e., with various quaternization ratios and (B) with fixed amounts of quaternized cross-linking agent (0.1 mmol) and various amounts of comonomer. All the measurements of zeta potential were performed at 25 °C. The pH of the obtained ionic microgels was measured to be 7.04 ± 0.07.

PNI6 and PNI4 ionic microgels, respectively (Figure 4). In other words, the volume changes of the PNI6 and PNI4 ionic microgels were ca. 816 and 468 times when the solution temperature was increased from 25 to 60 °C. However, the swelling ratios of PNP4 ionic microgels were much smaller than those of PNI6 and PNI4 ionic microgels. It was understandable because the monomer VIM was hydrophilic and the monomer of 4VP was hydrophobic in nature. Furthermore, the swelling ratios of PNI6 ionic microgels were higher than those of PNI4 ionic microgels at the same concentration of VIM and quaternization ratio. Because the cross-linking agent of 1,6-dibromohexane had a longer carbon chain than that of 1, 4-dibromobutane, the longer chain between the two cross-linking points of the microgel networks would allow the swelling of the networks to a larger extent than those networks with shorter chains, like PNI4 ionic microgels. On the other hand, the swelling ratios of PNI6 and PNI4 series of thermosensitive ionic microgels increased with raising the concentration of VIM when the amounts of the quaternization cross-linking agents were fixed. Because VIM was hydrophilic, increasing the content of hydrophilic comonomer will lead to the increase of swelling ratio for the P(NIPAm-*co*-VIM) microgels (cf. Table 1). The highest swelling ratio obtained in the present work could reach up to ca. 3490 for the PNI6-5# microgels. On the contrary, the swelling ratios of the PNP4 series of thermosensitive ionic microgels decreased with raising the concentration of hydrophobic 4VP when the amounts of the quaternization cross-linking agents were fixed (cf. Table 1). These results indicated that the swelling properties of the obtained thermosensitive ionic microgels could be tuned by selecting the proper comonomer, the content of comonomer, the quaternization cross-linking agents, and the quaternization ratio.

The zeta potentials of the PNI6, PNI4, and PNP4 series of thermosensitive ionic microgels were also measured, as shown in Figure 5. As was expected, the zeta potentials of the three series of ionic microgels were positive and increased linearly with the quaternization ratio increasing from 1/2 to 1 (Figure 5A). The positive zeta potential could be attributed to the quaternary comonomers of the obtained ionic microgels. The linear increase of zeta potential with feeding quaternization ratio increasing from 1/2 to 1 also suggested that the dibromide cross-linking agents almost completely reacted with the tertiary amines of the comonomers during the radical copolymerization, which is consistent with the results of Volhard's titration (cf. Table 3). The ionic microgels with feeding quaternization ratio of 2 were also prepared, and the corresponding zeta potentials were found to be similar with those with a feeding quaternization ratio of 1 (Figure 5A), which indicate that the degrees of quaternization had reached saturation for the comonomer (VIM or 4VP) with the feeding quaternization ratio of 2. The hydrodynamic radius R_h, swelling ratios, and TEM results of the thermosensitive ionic microgels with feeding quaternization ratio of 2, i.e., PNI4-6#, PNI6-6#, and PNP4-6# microgels, were summarized in Table 1 and Figure S6 (Supporting Information). As expected, the PNI4-6#, PNI6-6#, and PNP4-6# microgls had smaller sizes when compared with the corresponding microgels with feeding quaternization ratio of 1 because more hydrophobic dibromides could be incorporated within the microgels via quaternization. In other words, there were some single-ended quaternized hydrophobic dibromides in the microgels in these cases. Furthermore, the zeta potentials of PNI6, PNI4, and PNP4 were almost the same with various comonomer concentrations when the amounts of quaternized cross-linking agents were fixed, as shown in Figure 5B. These results might suggest that the quaternary N of the comonomer dominated the zeta potentials of the obtained thermosensitive ionic microgels.

The radius of gyration $\langle R_g \rangle$ of the obtained thermosensitive ionic microgels was also measured by static light scattering (SLS) at 25 °C. The SLS data could be well described by Guinier-type plots of $\ln I(q)^{-1} \sim q^2$ as shown in Figure S7 (Supporting Information), where I is the scattering intensity and $q = (4\pi n/\lambda)\sin(\theta/2)$, with λ, n, and θ being the wavelength of the laser light in vacuum (here λ = 637 nm), the refractive index of solvent, and the scattering angle, respectively. $\langle R_g \rangle$ could be then calculated from the slope of $\ln I(q)^{-1} \sim q^2$ via the equation given as

$$\ln I(q)^{-1} = \ln I(0)^{-1} + \frac{\langle R_g \rangle^2}{3} q^2 \quad (1)$$

Table 1 summarized the $\langle R_g \rangle$ and corresponding ratio of $\langle R_g \rangle / \langle R_h \rangle$ for the three series of thermosensitive ionic microgels studied here. The value of $\langle R_g \rangle / \langle R_h \rangle$ could reflect the conformation and architecture of a polymer chain in solution or the cross-linking density distribution of the microgels.[47,69−72] For example, $\langle R_g \rangle / \langle R_h \rangle$ values vary in the range of 1.50−1.78

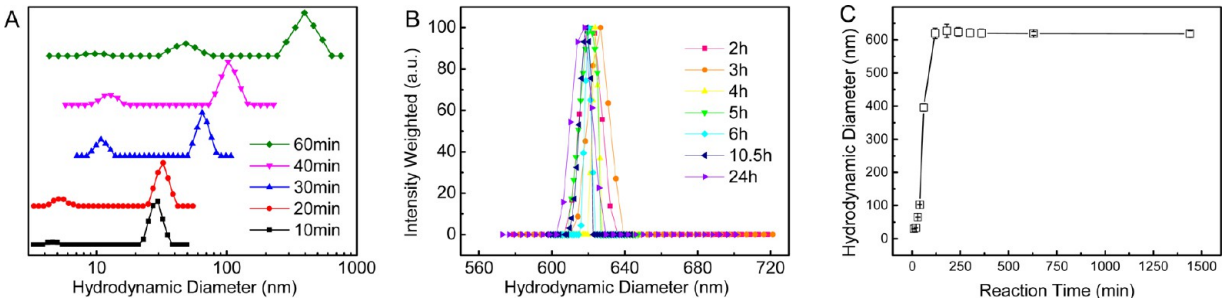

Figure 6. Variation of the hydrodynamic size and size distribution of PNI4-4# microgels by DLS at different polymerization times. (A) 10−60 min, (B) 2−24 h, (C) the variation of hydrodynamic diameters measured as a function of reaction time (10 min−24 h). All the DLS measurements were performed at 25 °C.

Scheme 2. Formation Mechanism of the Ionic Microgels

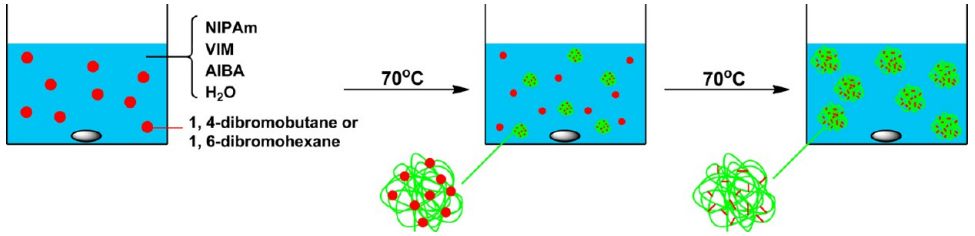

for random polymer coils, depending on the solvent quality. For uniform hard spheres, $\langle R_g\rangle/\langle R_h\rangle$ is 0.778. For thermosensitive PNIPAm microgels with inhomogenous cross-linking network structures, $\langle R_g\rangle/\langle R_h\rangle$ usually had the value of 0.55−0.6.[70,73] However, for the PNIPAm-related microgels made by postcross-linking reaction of linear cross-linkable copolymers, $\langle R_g\rangle/\langle R_h\rangle$ had the value of 0.74−0.87 reported by Kuckling et al.[47] and of 0.77−0.96 reported by Du et al.,[49] indicating that the microgels made by postcross-linking had more homogeneous cross-linked structures. The $\langle R_g\rangle/\langle R_h\rangle$ values of the PNI4, PNI6, and PNP4 series of thermosensitive ionic microgels at 25 °C varied in the range of 0.51−0.89, depending on the type and amount of comonomer and quaternized cross-linking agent. For PNI6 and PNI4 microgels, $\langle R_g\rangle/\langle R_h\rangle$ values increased from 0.57 and 0.52 to 0.81 and 0.75, respectively, when the quaternization ratios increased from 1/2 to 1 with fixed amounts of comonomer VIM. These results indicated that the increase of quaternization cross-linking density led to the more homogeneous microstructures of the PNI6 and PNI4 ionic microgels. After quaternization reaction, the hydrophilic pyridinium cations made the microstructure of ionic microgels more homogeneous. However, for PNP4 microgels, $\langle R_g\rangle/\langle R_h\rangle$ values decreased from 0.69 to 0.56 when the quaternization ratios increased from 1/2 to 1 with fixed amounts of comonomer 4VP, which might be due to the hydrophobic nature of 4VP. Furthermore, $\langle R_g\rangle/\langle R_h\rangle$ values of the ionic microgels decreased with increasing amounts of comonomer (VIM or 4VP) when the quaternization ratio was fixed (cf. Table 1). These results indicated that the ionic microgels with more homogeneous network structures could be obtained by selecting proper comonomer, the content of comonomer, and the quaternization ratio.

3.2. Formation Mechanism of the Ionic Microgels. To study the formation mechanism of the ionic microgels, the variation of the hydrodynamic size and size distribution of microgels with sample code of PNI4-4# was monitored by DLS via direct sampling of the product at different polymerization times. As shown in Figure 6, a clear shift of the hydrodynamic size toward large size was observed. Multimodal size distribution was found at the beginning of the reaction, and oligomeric products can be detected at the early stage of the polymerization (Figure 6A). After 2 h, the hydrodynamic size was almost unchanged, and the size distribution transformed to unimodal (Figures 6B and 6C). The evolution of the hydrodynamic size and size distribution clearly indicates that quaternization cross-linked microgels could be obtained after 2 h. To complete the polymerization and quaternization reaction, 6 h was chosen as the reaction time.

For our system, the monomers (NIPAm and VIM) and initiator (AIBA) are well soluble in water. However, dibromides (1,4-dibromobutane or 1,6-dibromohexane) are not soluble in water. It means that monomers and cross-linking molecules were in different phases at the beginning of the polymerization. As the reaction temperature increased to 70 °C (>LCST), NIPAm copolymerized with VIM and began to form hydrophobic particles. The hydrophobic particles improved the solubility of dibromides, and the quaternized cross-linking reaction took place within the particles. For PNP4 microgels, hydrophobic 4VP could be analogous to the dibromides. The schematic representation of the polymerization process was illustrated in Scheme 2.

To further study the formation mechanism of the ionic microgels, the fabrication of microgels was also attempted at room temperature. Experimental conditions were described in the Experimental Section, and the feed ratio was the same as that of PNI6-4# microgels. The variation of the hydrodynamic size and size distribution of samples were monitored by DLS by direct sampling of product at different polymerization times (see Supporting Information Figure S8). Clearly, there is no difference between the samples reacted for 6 h and 4 days. Before reaction, the solution was transparent with insoluble dibromides floating on the surface. After 4 days, the phenomenon had not changed. GPC and ^{1}H NMR results indicated that only linear copolymers were obtained (M_n = 2.7 × 10^4, PDI = 2.0, see Supporting Information Figure S9).

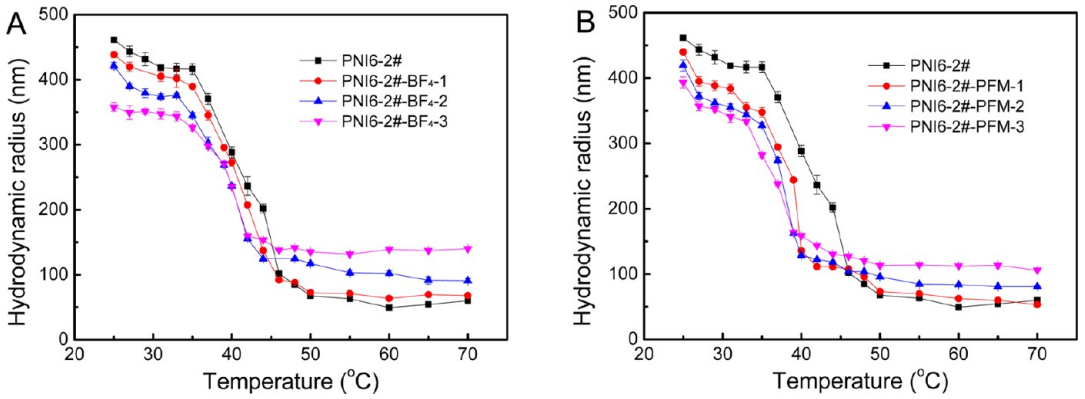

Figure 7. Hydrodynamic radii of the PNI6−2# thermosensitive ionic microgels measured by DLS as a function of measuring temperature before and after anionic exchange reactions with various concentrations of salts (A) BF_4K and (B) PFM-Li. The detailed experimental conditions were given in Table 2.

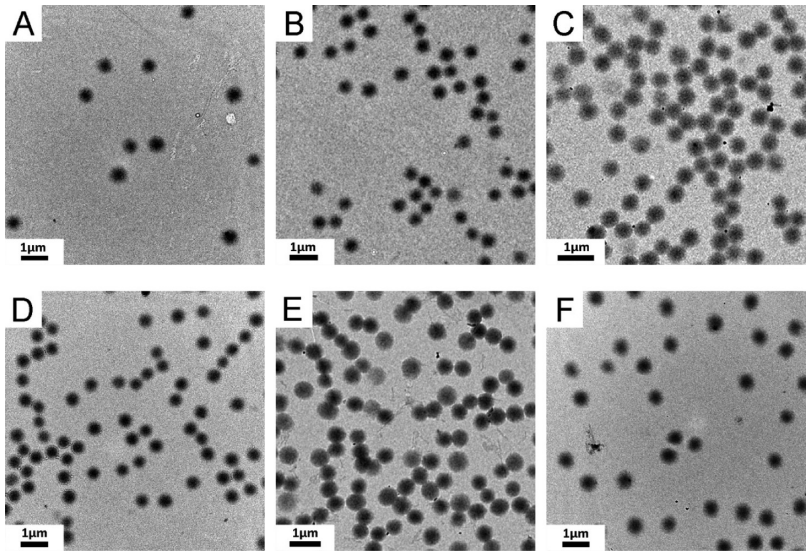

Figure 8. TEM images of PNI6-2# thermosensitive ionic microgels after anionic exchange reactions with various concentrations of BF_4K and PFM-Li. (A) PNI6-2#−BF_4-1, (B) PNI6-2#−BF_4-2, (C) PNI6-2#−BF_4-3, (D) PNI6-2#−PFM-1, (E) PNI6-2#−PFM-2, and (F) PNI6-2#−PFM-3.

The key factor for the formation of the resultant ionic microgels is the high reaction temperature. It has three important functions: (1) the high reaction temperature promoted initiator decomposition to cause the polymerization of monomers; (2) PNIPAm chains became hydrophobic and insoluble and formed aggregates above its LCST, which was helpful to improve the solubility of hydrophobic cross-linking agents; (3) the high reaction temperature accelerated the quaternization reaction. In addition, we also attempted to use the hydrophilic dibromides, ethanediol bis(2-bromoacetate), as cross-linking agents to synthesize the ionic microgels. However, it failed, and no microgel was obtained. The reason might be that the hydrophilic dibromides dispersed uniformly in solution so that the concentration of cross-linking agents in the hydrophobic P(NIPAm-*co*-VIM) particles formed at elevated temperature was too low to form a cross-linked network. This phenomenon further illustrates that the formation mechanism of the ionic microgels proposed above in Scheme 2 is reasonable.

3.3. Anion Exchange Reaction of the Thermosensitive Ionic Microgels. Since the obtained thermosensitive ionic microgels possessed quaternized VIM or 4VP moieties, the microgels also exhibited the typical characteristic of ionic liquid or polymeric ionic liquid (PIL). The counteranions of quaternized imidazole (imidazolium) and pyridine (pyridinium) moieties could be altered via anion exchange reaction. Here, BF_4K and PFM-Li were used as the sources of anion, and the P(NIPAm-*co*-VIM)/1,6-dibromohexane microgels with sample code of PNI6-2# were chosen to demonstrate the anion exchange reactions with BF_4K and PFM-Li. The detailed experimental conditions of anion exchange reactions were summarized in Table 2.

Figure 7 shows the hydrodynamic radii of the PNI6-2# thermosensitive ionic microgels before and after the anion exchange reaction as a function of measuring temperature. The anion exchange reaction with more hydrophobic anionic groups led to the decrease of hydrodynamic radius, VPTT, and swelling ratios of the corresponding microgels. These results had similarities with the features of PILs. The most notable feature of PILs is that the nature of the counteranion strongly influences their solubility behavior.[17,61,74] Mecerreyes[23] summarized that PILs with imidazolium, alkylammonium, pyridinium, or guanidinium cationic backbones were soluble in water bearing halide anions. However, when the halide anions were substituted by hydrophobic anions, the PILs were not soluble in water anymore but became soluble in organic

dx.doi.org/10.1021/am500291n | ACS Appl. Mater. Interfaces 2014, 6, 4498−4513

Table 4. Solubility Tests and Thermal Parameters of PNI6-4# Thermosensitive Ionic Microgels before and after Anion Exchange Reactions

	solubility test[a]				thermal parameters		
sample code	water	MeOH	acetone	THF	$T_{d,5wt\%}$ (°C)[b]	T_{max} (°C)[c]	Y_c (wt %)[d]
PNI6-4#	+	−	−	−	319.4	412.6	1.3
PNI6-4#−BF_4	+	−	−	−	334.6	413.3	2.8
PNI6-4#−PFM	+	+	+	+	317.0	413.3	5.3

[a]+: the microgels could disperse well in the solvent. −: the microgels could not disperse well in the solvent. [b]$T_{d,5wt\%}$ is the decomposition temperature of 5 wt % weight loss, which indicates the apparent thermal stability of the microgels. [c]T_{max} indicates the temperature of maximum decomposition rate. [d]Determined at 800 °C.

solvents.[23] Mecerreyes et al.[17] also reported a new type of PIL microgels prepared by the concentrated emulsion polymerization of the ionic liquid monomer, 1-vinyl-3-ethylimidazolium bromide (ViEtIm$^+$Br$^-$), with *N*,*N*-dimethylenebisacrylamide (BIS) as the cross-linking agent. The obtained microgels having bromide anions could be dispersed in water and methanol (MeOH). After the anion exchange reaction, the microgels bearing hydrophobic counterions such as $CF_3SO_3^-$, $(CF_3SO_3)_2N^-$, and $(CF_3CF_2SO_2)_2N^-$ could swell in nonpolar solvents such as acetone and tetrahydrofuran (THF).[17] These PIL microgels showed a larger size after anion exchange than the precursor microgels with bromide anions.[17] In the present work, the hydrodynamic radius of microgels decreased after the anion exchange reaction with more hydrophobic anions. More hydrophobic anions exchanged inside the ionic microgels resulting in the smaller hydrodynamic radius of the ionic microgels. Furthermore, unlike some PILs that will be precipitated in the aqueous solutions with hydrophobic counteranions, the PNI6-2# thermosensitive ionic microgels showed good stability in aqueous solution and also maintained the thermosensitive properties after the anion exchange reaction (Figure 7), which might be ascribed to the hydrophilic PNIPAm network segments. Similar results were obtained for the hydrodynamic radii of the PNI4-2# thermosensitive ionic microgels before and after the anion exchange reaction as a function of measuring temperature. The anion exchange reaction with more hydrophobic anionic groups led to the decrease of hydrodynamic radius, VPTT, and swelling ratios of the corresponding microgels, as shown in Figure S10 (Supporting Information).

To get insight into the microstructures of the PNI6-2# thermosensitive ionic microgels before and after anion exchange reaction in aqueous solution, the ratios of $\langle R_g \rangle / \langle R_h \rangle$ were also measured and included in Table 2. The anion exchange reaction with more hydrophobic anionic groups led to the increase of $\langle R_g \rangle / \langle R_h \rangle$ values, which might indicate that the hydrophobic anionic counterions led to the more compacted architecture of the PNI6-2# thermosensitive ionic microgels. Figure 8 shows the TEM images of the PNI6-2# thermosensitive ionic microgels after anion exchange reaction with various concentrations of BF_4K and PFM-Li. The PNI6-2# microgels maintained the spherical shape with narrow size distribution after anion exchange. The average diameters of PNI6-2# microgels calculated from TEM images were listed in Table 2. After the anion exchange reaction, the dried microgels showed a larger size than those of the precursor microgels with bromide anions, which were similar to Mecerreyes et al.'s results.[17] Figure S11 (Supporting Information) shows that the PNI6-2# ionic microgels exhibited a narrow size distribution in aqueous solution at 25 °C before and after anion exchange reactions as measured by DLS, which was consistent with the size distribution of dried microgels obtained by TEM.

To further demonstrate the effect of anion exchange on the properties of the resultant thermosensitive ionic microgels, the anion exchange reactions were carried out with PNI6-4# microgels and excess amounts of BF_4K and PFM-Li, respectively (cf. Table 2). After anion exchange reactions, the solubility of the obtained PN6-4#−BF_4 and PNI6-4#−PFM microgels in various solvents with different polarities, namely, water, methanol (MeOH), acetone, and tetrahydrofuran (THF), was tested. The results of solubility tests were summarized in Table 4 and Figure S12 (Supporting Information). Before anion exchange, the PNI6-4# thermosensitive ionic microgels with the bromide ion as the counteranion could well disperse in water but precipitate in the other three solvents, i.e., MeOH, acetone, and THF. After anion exchange reaction with BF_4K, the PN6-4#−BF_4 microgels with BF_4^- as the counteranion also showed the same results. However, the PNI6-4#−PFM microgels with trifluoromethyl sulfonate (PFM^-) as the counteranions showed good solubility in all solvents tested because of the synergism between the hydrophilic PNIPAm segments and the hydrophobic counteranion PFM^-. These results revealed that it was possible to fabricate the thermosensitive ionic microgels, which could not only well disperse in water but also have good solubility in other organic solvents. The organically soluble thermosensitive ionic microgels might have potential applications in many technical fields.

Thermal stabilities of the PNI6-4# thermosensitive ionic microgels with different anions, i.e., Br^-, BF_4^-, and PFM^-, were also investigated by thermogravimetric analysis (TGA). The PNI6-4# thermosensitive ionic microgels before and after anion exchange reactions with BF_4K and PFM-Li were freeze-dried and then subjected to thermogravimetric analysis. Figure 9 shows the TGA curves of PNI6-4#, PN6-4#−BF_4, and PNI6-4#−PFM ionic microgels. The 5 wt % decomposition temperature ($T_{d,5wt\%}$), the maximum decomposition temperature (T_{max}), and char residue at 800 °C (Y_c) were determined and summarized in Table 4. $T_{d,5wt\%}$ is the decomposition temperature of 5 wt % weight loss, which indicates the apparent thermal stability of the microgels. T_{max} indicates the temperature of maximum decomposition rate. It can be seen from Figure 9 and Table 4 that the anion exchange reaction did not affect the T_{max} values of the PNI6-4# ionic microgels. However, $T_{d,5wt\%}$ values of PNI6-4# ionic microgels with BF_4^- as the counteranion was significantly higher than Br^- ones. After anion exchange reaction, char residue values Y_c of the PNI6-4# ionic microgels with BF_4^- and PFM^- as counteranions were also higher than Br^-, indicating that the structure of the counteranion would influence the thermal stability of the ionic microgels. The values of Y_c of the PNI6-4# ionic microgels

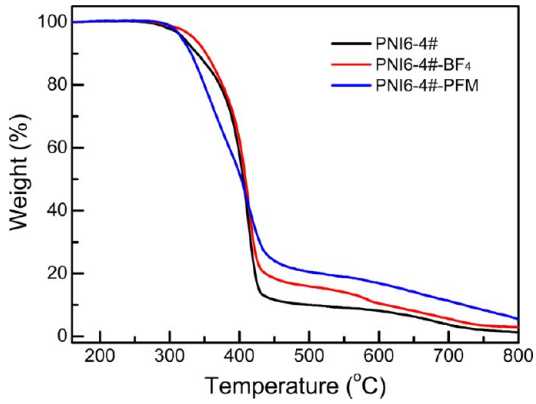

Figure 9. TGA curves of the PNI6-4# thermosensitive ionic microgels before and after anion exchange reactions with BF_4K and PFM-Li.

significantly increased from 1.3 wt % for the microgels with Br^- as a counteranion to 2.8 wt % and 5.3 wt % for the microgels with BF_4^- and PFM^- as counteranions, respectively. Mecerreyes et al.[17] reported that the nature of the counteranions had a strong influence on the thermal stability of PIL microgels, and the anion structure X^- influenced the thermal stability of poly(ViEtIm$^+X^-$) microgels with BIS as the cross-linking agent in the order of $(CF_3SO_2)N^- > (CF_3CF_2SO_2)_2N^- > CF_3SO_3^- > C_{12}H_{25}C_6H_4SO_3^- > BF_4^- > Br^-$. In the present work, although the obtained thermosensitive ionic microgels only contained less than 15% of PIL moieties, the nature of counteranions indeed exhibited strong influences on their solubility, thermosensitive behavior, and thermal stability. The results of Figure 9 indicated that the obtained thermosensitive ionic microgels exhibited thermal stability with counteranions in the order of $CF_3SO_3^- > BF_4^- > Br^-$, which was consistent with those observed by Mecerreyes et al.[17]

3.4. Encapsulation and Release of Dyes. As has been discussed above, the obtained thermosensitive ionic microgels contained the quaternized VIM or 4VP moieties and hence exhibited a unique feature of PILs. The counteranion of the thermosensitive ionic microgels could be altered via the anion exchange reactions. Here, it was further demonstrated that the obtained thermosensitive ionic microgels could be used to efficiently encapsulate and release water-soluble anionic dyes via the anion exchange reactions, as shown in Scheme 1. Methyl orange (MO) was used as the model of water-soluble anionic dyes, and the PNI4 series of thermosensitive ionic microgels were chosen to demonstrate the encapsulation and controlled release of MO in aqueous solutions. The detailed procedures of encapsulation and release of MO were described in the Experimental Section. Table 5 summarized the experimental conditions of the encapsulation of MO. After dialysis in deionized water for 1 week, the PNI4-4# thermosensitive ionic microgels in the dialysis tube exhibited orange colors, and the water in the beaker was transparent and clear, as shown in Figure 10A. This indicated that MO was successfully encapsulated within the ionic microgels.

Figures 10B and 10C show the UV absorption spectra of MO-encapsulated PNI4 series of microgels and the pure MO solutions. The MO-encapsulated PNI4 microgels showed UV–visible spectra with shape and absorption maximum (ca. 460 nm) identical to those of pure MO solutions. Sawamoto et al.[75] reported the synthesis of a cation-condensed star polymer by the linking reaction of a poly(ethylene glycol) (PEG) macroinitiator with a quaternary ammonium cation-carrying linking agent in ruthenium-catalyzed living radical polymerization. Such cation-condensed microgel–core star polymers with PEG-based arms could be used to encapsulate and stimuli-responsively release hydrophilic and anionic dyes in water. They observed that the encapsulated MO exhibited a blue shift of the absorption maximum to 415 nm from that of 460 nm for pure MO aqueous solution, which was attributed to the MO aggregation formed in the core of the star polymer with locally concentrated quaternary ammonium cations.[75] The identical UV absorption spectra observed here might suggest that the encapsulated MO molecules were uniformly distributed within the PNI4 microgels, and there was no aggregation. It might also suggest that the quaternized VIM moieties were uniformly distributed inside the obtained thermosensitive ionic microgels via the in situ quaternization cross-linking reaction. In other words, the quaternized cross-linking network structures of the obtained thermosensitive ionic microgels were relatively uniform. Figure 10B shows that the amounts of MO encapsulated within the PNI4-4# microgels increased with increasing the feeding molar ratios of [MO] to [VIM$^+$]. The actual amounts of MO encapsulated within the PNI4-4# microgels were about 0.8, 1.5, 2.0, and 2.8 mg for [MO]:[VIM$^+$] of 3/10, 5/10, 10/10, and 15/10, respectively (cf. Table 5). The encapsulation efficiency (EE%) and saturation encapsulation efficiency (SEE%) were also listed in Table 5. The capacities of the obtained thermosensitive ionic microgels for the encapsulation of anionic MO dye were dependent on the quaternization ratio of the microgels, i.e., the content of quaternized VIM moieties in the microgels, as shown in Figure 10C and Table 5. The PNI4 microgels with higher quaternization ratio could encapsulate higher amounts of MO when the concentration of MO was fixed. The encapsulation capacities of MO for PNI4-2#–MO4, PNI4-3#–MO4, and

Table 5. Composition and Properties of MO-Encapsulated Thermosensitive Ionic Microgels

		feed amount						
sample code	microgels	PNI4 (mg)	$Q_{t,MO}$[a] (mg)	molar ratio: MO/VIM$^+$	$Q_{s,MO}$[b] (mg)	$Q_{e,MO}$[c] (mg)	EE[d] (%)	SEE[e] (%)
PNI4-4#–MO1	PNI4–4#	10	1.0	3/10	1.0	0.8	80.0	80.0
PNI4-4#–MO2			1.7	5/10	1.7	1.5	88.2	88.2
PNI4-4#–MO3			3.4	10/10	3.4	2.0	58.8	58.8
PNI4-4#–MO4			5.1	15/10	3.4	2.8	54.9	82.4
PNI4-2#–MO4	PNI4-2#		5.1	3/1	1.7	0.6	11.8	35.3
PNI4-3#–MO4	PNI4-3#		5.1	9/4	2.3	1.5	29.4	65.2

[a] $Q_{t,MO}$: the content of MO initially added. [b] $Q_{s,MO}$: the theoretical maximum MO content in the MO-encapsulated PNI4 microgels based on the content of MO initially added, i.e., the saturation MO content. [c] $Q_{e,MO}$: the actual MO content in the MO-encapsulated PNI4 microgels. [d] EE%: encapsulation efficiency, EE% = $(Q_{e,MO}/Q_{t,MO}) \times 100$ (%). [e] SEE%: saturation encapsulation efficiency, SEE% = $(Q_{e,MO}/Q_{s,MO}) \times 100$ (%).

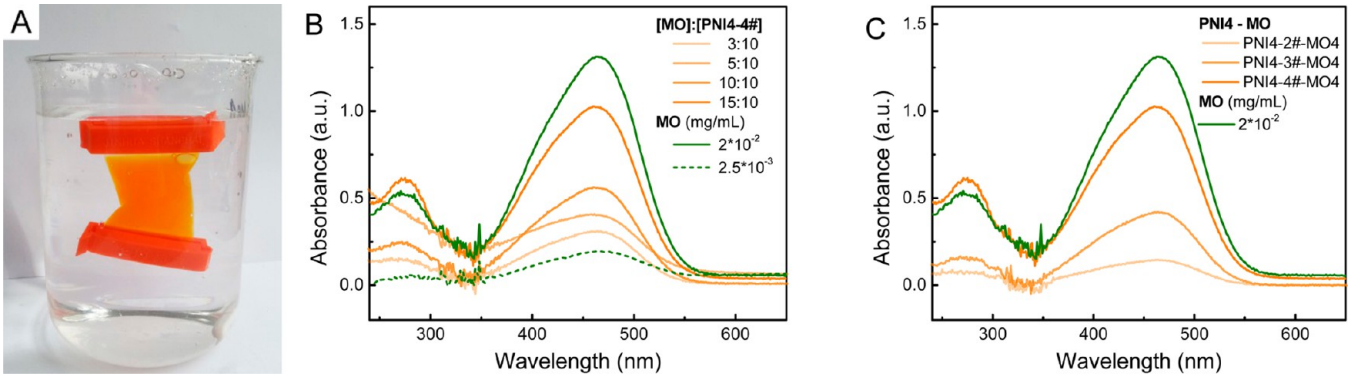

Figure 10. (A) Photoimage of PNI4-4#−MO4 microgels with encapsulation of MO. (B) UV absorption spectra of MO-encapsulated PNI4-4# microgels with various feeding molar ratios of MO to quaternized imidazole moieties of PNI4-4#, i.e., [MO]/[VIM$^+$] = 3/10, 5/10, 10/10, and 15/10, respectively. (C) UV absorption spectra of MO-encapsulated PNI4 microgels with fixed amounts of MO and various quaternization ratios of 1/2 (PNI4-2#), 2/3 (PNI4-3#), and 1 (PNI4-4#). The concentrations of MO-encapsulated microgel suspensions were 0.05 mg/mL. The UV absorption spectra of pure MO solutions with concentration of 2×10^{-2} mg/mL and 2.5×10^{-3} mg/mL were also included.

PNI4-4#−MO4 microgels with quaternization ratios of 1/2, 2/3, and 1 were in the order of PNI4-4#−MO4 > PNI4-3#−MO4 > PNI4-2#−MO4 (Figure 10C). The excess MO could increase the saturation encapsulation efficiency (SEE%) of the microgels. The results of Figure 10 showed that the obtained thermosensitive ionic microgels with quaternary ammonium cations could encapsulate the anion dyes in aqueous solutions in an efficient and versatile way.

The encapsulated MO could then be released from the microgels via the anion exchange reaction. By dialyzing the MO-encapsulated microgels in 0.1 M NaCl aqueous solution, MO was gradually released from the microgels, as shown in Figure 11. For about 400 min, about 90% of the encapsulated

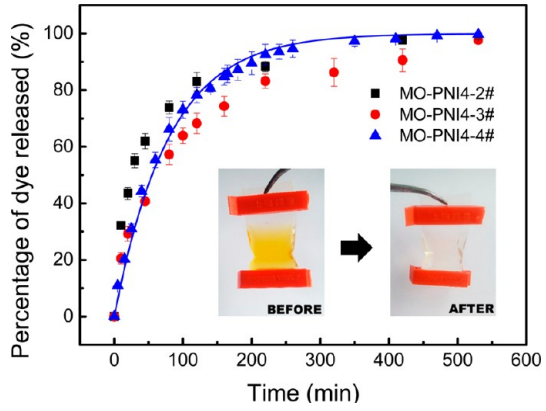

Figure 11. Release profiles of MO from the MO-encapsulated PNI4-2#−MO4, PNI4-3#−MO4, and PNI4-4#−MO4 microgels as a function of dialysis time in 0.1 M NaCl aqueous solutions.

MO was released into the NaCl aqueous solutions for the MO-encapsulated PNI4-2#−MO4, PNI4-3#−MO4, and PNI4-4#−MO4 microgels. The release rates of MO were almost the same for the three microgels. After complete release, the colors of the microgel dispersions turned from orange to transparent, as shown in the inset of Figure 11. The release kinetic of MO from the PNI4 series of ionic microgels in NaCl aqueous solution could be well described by the first-order equation given as

$$-\ln\left(1 - \frac{M_t}{M_\infty}\right) = \frac{k_r t}{2.303} \quad (2)$$

where M_t is the amount of the encapsulated compound release at time t; M_∞ is the amount of the encapsulated compound release after infinite time; k_r is the first-order rate constant; and t is the time. This model is used to describe the release of water-soluble drug or dye.[76,77] The fit of eq 2 gave the first-order rate constant k_r of 2.96×10^{-2} min^{-1} for the release of MO from the PNI4 series of ionic microgels in NaCl aqueous solution. These results suggested that the thermosensitive ionic microgels obtained in the present work might have potential and promising applications in dye-loading and controlled release systems and the treatment of wastewater with dye contamination. Such thermosensitive ionic microgels with cationic moieties and anionic counterions could be suitable for the treatment of anionic dye via anionic exchange reaction.

4. CONCLUSIONS

A type of thermosensitive ionic microgels was successfully obtained via in situ quaternization cross-linking of quaternizable comonomer like 1-vinylimidazole and 4-vinylpyridine with dibromides like 1,4-dibromobutane and 1,6-dibromohexane during the surfactant-free emulsion copolymerization of thermosensitive monomer *N*-isopropylacrylamide and the comonomer at 70 °C. The obtained microgels were spherical in shape with narrow size distribution and exhibited thermosensitive behavior and unique features of PILs in aqueous solution, of which the counteranions of the microgels could be changed by anion exchange reaction with BF_4K or lithium trifluoromethyl sulfonate (PFM-Li). After anion exchange reaction, the microgels were stable in aqueous solution. Especially, the microgels with PFM$^-$ as the counteranion could be also well dispersed in MeOH, acetone, and THF. The sizes and thermosensitive behavior of the microgels could be well tuned by controlling the quaternization ratio, the type of comonomers, dibromides, and counteranions. The microgels showed superior swelling properties in aqueous solution. Furthermore, such ionic microgels also showed capabilities to encapsulate and release the anionic dyes like methyl orange in aqueous solution, which could be also tuned by selecting the proper comonomer, the content of

comonomer, the quaternization cross-linking agents, and the quaternization ratio.

■ ASSOCIATED CONTENT

Supporting Information

TEM images of PNI6 and PNP4 series of thermosensitive ionic microgels, additional SLS and DLS data, ^{1}H NMR and GPC data, photo pictures of solubility tests. This material is available free of charge via the Internet at http://pubs.acs.org.

■ AUTHOR INFORMATION

Corresponding Author

*E-mail: duby@zju.edu.cn.

Notes

The authors declare no competing financial interest.

■ ACKNOWLEDGMENTS

We greatly thank Prof. Yingfeng Tu at Soochow University for his help on laser light scattering experiments. The authors thank the National Natural Science Foundation of China (Nos. 21274129 and 21322406), the Fundamental Research Funds for the Central Universities, and Zhejiang University K.P. Chao's High Technology Development Foundation for financial support.

■ REFERENCES

(1) Walden, P. Über die Molekulargröße und elektrische Leitfähigkeit einiger geschmolzener Salze. *Bull. Acad. Impér. Sci. St. Pétersbourg* **1914**, *8*, 405−422.

(2) Yoke, J. T., III; Weiss, J. F.; Tollin, G. Reactions of triethylamine with copper (I) and copper (II) halides. *Inorg. Chem.* **1963**, *2*, 1210−1216.

(3) Swain, C. G.; Ohno, A.; Roe, D. K.; Brown, R.; Maugh, T. Tetrahexylammonium benzoate, a liquid salt at 25. degree., a solvent for kinetics or electrochemistry. *J. Am. Chem. Soc.* **1967**, *89*, 2648−2649.

(4) Kubisa, P. Application of ionic liquids as solvents for polymerization processes. *Prog. Polym. Sci.* **2004**, *29*, 3−12.

(5) Suzuki, K.; Yamaguchi, M.; Hotta, S.; Tanabe, N.; Yanagida, S. A new alkyl-imidazole polymer prepared as an inonic polymer electrolyte by in situ polymerization of dye sensitized solar cells. *J. Photochem. Photobiol., A* **2004**, *164*, 81−85.

(6) Li, F.; Cheng, F.; Shi, J.; Cai, F.; Liang, M.; Chen, J. Novel quasi-solid electrolyte for dye-sensitized solar cells. *J. Power Sources* **2007**, *165*, 911−915.

(7) Zhang, Y.; Zhao, L.; Patra, P. K.; Hu, D.; Ying, J. Y. Colloidal poly-imidazolium salts and derivatives. *Nano Today* **2009**, *4*, 13−20.

(8) Marcilla, R.; Alberto Blazquez, J.; Rodriguez, J.; Pomposo, J. A.; Mecerreyes, D. Tuning the solubility of polymerized ionic liquids by simple anion-exchange reactions. *J. Polym. Sci., Part A: Polym. Chem.* **2004**, *42*, 208−212.

(9) Marcilla, R.; Alcaide, F.; Sardon, H.; Pomposo, J. A.; Pozo-Gonzalo, C.; Mecerreyes, D. Tailor-made polymer electrolytes based upon ionic liquids and their application in all-plastic electrochromic devices. *Electrochem. Commun.* **2006**, *8*, 482−488.

(10) Kawano, R.; Katakabe, T.; Shimosawa, H.; Nazeeruddin, M. Solid-state dye-sensitized solar cells using polymerized ionic liquid electrolyte with platinum-free counter electrode. *Phys. Chem. Chem. Phys.* **2010**, *12*, 1916−1921.

(11) Wang, G.; Wang, L.; Zhuo, S.; Fang, S.; Lin, Y. An iodine-free electrolyte based on ionic liquid polymers for all-solid-state dye-sensitized solar cells. *Chem. Commun.* **2011**, *47*, 2700−2702.

(12) Lin, B.; Qiu, L.; Qiu, B.; Peng, Y.; Yan, F. A soluble and conductive polyfluorene ionomer with pendant imidazolium groups for alkaline fuel cell applications. *Macromolecules* **2011**, *44*, 9642−9649.

(13) Lin, B.; Qiu, L.; Lu, J.; Yan, F. Cross-linked alkaline ionic liquid-based polymer electrolytes for alkaline fuel cell applications. *Chem. Mater.* **2010**, *22*, 6718−6725.

(14) Pozo-Gonzalo, C.; Marcilla, R.; Salsamendi, M.; Mecerreyes, D.; Pomposo, J. A.; Rodríguez, J.; Bolink, H. J. PEDOT: Poly (1-vinyl-3-ethylimidazolium) dispersions as alternative materials for optoelectronic devices. *J. Polym. Sci., Part A: Polym. Chem.* **2008**, *46*, 3150−3154.

(15) Kim, T.; Suh, M.; Kwon, S.; Lee, T.; Kim, J.; Lee, Y.; Kim, J.; Hong, M.; Suh, K. Poly (3, 4-ethylenedioxythiophene) derived from poly (ionic liquid) for the use as hole-injecting material in organic light-emitting diodes. *Macromol. Rapid Commun.* **2009**, *30*, 1477−1482.

(16) Guo, J.; Qiu, L.; Deng, Z.; Yan, F. Plastic reusable pH indicator strips: preparation via anion-exchange of poly (ionic liquids) with anionic dyes. *Polym. Chem.* **2013**, *4*, 1309−1312.

(17) Marcilla, R.; Sanchez-Paniagua, M.; Lopez-Ruiz, B.; Lopez-Cabarcos, E.; Ochoteco, E.; Grande, H.; Mecerreyes, D. Synthesis and characterization of new polymeric ionic liquid microgels. *J. Polym. Sci., Part A: Polym. Chem.* **2006**, *44*, 3958−3965.

(18) Muldoon, M. J.; Gordon, C. M. Synthesis of gel-type polymer beads from ionic liquid monomers. *J. Polym. Sci., Part A: Polym. Chem.* **2004**, *42*, 3865−3869.

(19) Qiu, L.; Liu, B.; Peng, Y.; Yan, F. Fabrication of ionic liquid-functionalized polypyrrole nanotubes decorated with platinum nanoparticles and their electrocatalytic oxidation of methanol. *Chem. Commun.* **2011**, *47*, 2934−2936.

(20) Ishikawa, T.; Kobayashi, M.; Takahara, A. Macroscopic frictional properties of poly (1-(2-methacryloyloxy) ethyl-3-butyl imidazolium bis (trifluoromethanesulfonyl)-imide) brush surfaces in an ionic liquid. *ACS Appl. Mater. Interfaces* **2010**, *2*, 1120−1128.

(21) Jia, W.; Wu, Y.; Huang, J.; An, Q.; Xu, D.; Wu, Y.; Li, F.; Li, G. Poly (ionic liquid) brush coated electrospun membrane: a useful platform for the development of functionalized membrane systems. *J. Mater. Chem.* **2010**, *20*, 8617−8623.

(22) Ito, K.; Nishina, N.; Ohno, H. Enhanced ion conduction in imidazolium-type molten salts. *Electrochim. Acta* **2000**, *45*, 1295−1298.

(23) Mecerreyes, D. Polymeric ionic liquids: Broadening the properties and applications of polyelectrolytes. *Prog. Polym. Sci.* **2011**, *36*, 1629−1648.

(24) Azzaroni, O.; Brown, A. A.; Huck, W. T. Tunable wettability by clicking counterions into polyelectrolyte brushes. *Adv. Mater.* **2007**, *19*, 151−154.

(25) Men, Y.; Drechsler, M.; Yuan, J. Double-stimuli-responsive spherical polymer brushes with a poly (ionic liquid) core and a thermoresponsive shell. *Macromol. Rapid Commun.* **2013**, *34*, 1721−1727.

(26) Vijayakrishna, K.; Mecerreyes, D.; Gnanou, Y.; Taton, D. Polymeric vesicles and micelles obtained by self-assembly of ionic liquid-based block copolymers triggered by anion or solvent exchange. *Macromolecules* **2009**, *42*, 5167−5174.

(27) Wang, Z.; Lai, H.; Wu, P. Influence of PIL segment on solution properties of poly (N-isopropylacrylamide)-b-poly (ionic liquid) copolymer: micelles, thermal phase behavior and microdynamics. *Soft Matter* **2012**, *8*, 11644−11653.

(28) Hu, X.; Huang, J.; Zhang, W.; Li, M.; Tao, C.; Li, G. Photonic ionic liquids polymer for naked-eye detection of anions. *Adv. Mater.* **2008**, *20*, 4074−4078.

(29) Wu, G.; Jiang, Y.; Xu, D.; Tang, H.; Liang, X.; Li, G. Thermoresponsive inverse opal films fabricated with liquid-crystal elastomers and nematic liquid crystals. *Langmuir* **2010**, *27*, 1505−1509.

(30) Yan, F.; Texter, J. Solvent-reversible poration in ionic liquid copolymers. *Angew. Chem., Int. Ed.* **2007**, *46*, 2440−2443.

(31) Pelton, R. H.; Chibante, P. Preparation of aqueous lattices with N-isopropylacrylamide. *Colloids Surf.* **1986**, *20*, 247−256.

(32) Saunders, B. R.; Vincent, B. Microgel particles as model colloids: theory, properties and applications. *Adv. Colloid Interface Sci.* **1999**, *80*, 1−25.

(33) Pelton, R. Temperature-sensitive aqueous microgels. *Adv. Colloid Interface Sci.* **2000**, *85*, 1−33.
(34) Hoare, T.; Pelton, R. Engineering glucose swelling responses in poly (N-isopropylacrylamide)-based microgels. *Macromolecules* **2007**, *40*, 670−678.
(35) Benee, L.; Snowden, M.; Chowdhry, B. Novel gelling behavior of poly (N-isopropylacrylamide-co-vinyl laurate) microgel dispersions. *Langmuir* **2002**, *18*, 6025−6030.
(36) Bradley, M.; Vincent, B. Interaction of nonionic surfactants with copolymer microgel particles of NIPAM and acrylic acid. *Langmuir* **2005**, *21*, 8630−8634.
(37) Berndt, I.; Pedersen, J. S.; Richtering, W. Temperature-sensitive core-shell microgel particles with dense shell. *Angew. Chem., Int. Ed.* **2006**, *45*, 1737−1741.
(38) Bradley, M.; Vincent, B. Poly (vinylpyridine) core/poly (N-isopropylacrylamide) shell microgel particles: Their characterization and the uptake and release of an anionic surfactant. *Langmuir* **2008**, *24*, 2421−2425.
(39) Dalmont, H.; Pinprayoon, O.; Saunders, B. R. Study of pH-responsive microgels containing methacrylic acid: Effects of particle composition and added calcium. *Langmuir* **2008**, *24*, 2834−2840.
(40) Kleinen, J.; Richtering, W. Defined complexes of negatively charged multisensitive poly (N-isopropylacrylamide-co-methacrylic acid) microgels and poly (diallydimethylammonium chloride). *Macromolecules* **2008**, *41*, 1785−1790.
(41) Gan, D. J.; Lyon, L. A. Tunable swelling kinetics in core-shell hydrogel nanoparticles. *J. Am. Chem. Soc.* **2001**, *123*, 7511−7517.
(42) Kuckling, D.; Vo, C. D.; Wohlrab, S. E. Preparation of nanogels with temperature-responsive core and pH-responsive arms by photo-cross-linking. *Langmuir* **2002**, *18*, 4263−4269.
(43) Vo, C. D.; Kuckling, D.; Adler, H.-J.; Schönhoff, M. Preparation of thermosensitive nanogels by photo-cross-linking. *Colloid Polym. Sci.* **2002**, *280*, 400−409.
(44) Lyon, L. A.; Debord, J. D.; Debord, S. B.; Jones, C. D.; McGrath, J. G.; Serpe, M. J. Microgel colloidal crystals. *J. Phys. Chem. B* **2004**, *108*, 19099−19108.
(45) Zhang, J.; Xu, S.; Kumacheva, E. Polymer microgels: reactors for semiconductor, metal, and magnetic nanoparticles. *J. Am. Chem. Soc.* **2004**, *126*, 7908−7914.
(46) Nolan, C. M.; Reyes, C. D.; Debord, J. D.; García, A. J.; Lyon, L. A. Phase transition behavior, protein adsorption, and cell adhesion resistance of poly (ethylene glycol) cross-linked microgel particles. *Biomacromolecules* **2005**, *6*, 2032−2039.
(47) Kuckling, D.; Vo, C. D.; Adler, H.-J.; Völkel, A.; Cölfen, H. Preparation and characterization of photo-cross-linked thermosensitive PNIPAAm nanogels. *Macromolecules* **2006**, *39*, 1585−1591.
(48) Gupta, S.; Kuckling, D.; Kretschmer, K.; Choudhary, V.; Adler, H.-J. Synthesis and characterization of stimuli-sensitive micro- and nanohydrogels based on photocrosslinkable poly(dimethylaminoethyl methacrylate). *J. Polym. Sci., Part A: Polym. Chem.* **2007**, *45*, 669−679.
(49) Cao, Z.; Du, B.; Chen, T.; Nie, J.; Xu, J.; Fan, Z. Preparation and properties of thermo-sensitive organic/inorganic hybrid microgels. *Langmuir* **2008**, *24*, 12771−12778.
(50) Cao, Z.; Chen, T.; Guo, X.; Zhou, X.; Nie, J.; Xu, J.; Fan, Z.; Du, B. Synthesis and properties of organic-inorganic hybrid P (NIPAM-co-AM-co-TMSPMA) microgels. *Chin. J. Polym. Sci.* **2011**, *29*, 439−449.
(51) Chen, T.; Cao, Z.; Guo, X.; Nie, J.; Xu, J.; Fan, Z.; Du, B. Preparation and characterization of thermosensitive organic-inorganic hybrid microgels with functional Fe_3O_4 nanoparticles as crosslinker. *Polymer* **2011**, *52*, 172−179.
(52) Seiffert, S. Functional microgels tailored by droplet-based microfluidics. *Macromol. Rapid Commun.* **2011**, *32*, 1600−1609.
(53) Seiffert, S. Microgel capsules tailored by droplet-based microfluidics. *ChemPhysChem* **2013**, *14*, 295−304.
(54) Seiffert, S. Non-spherical soft supraparticles from microgel building blocks. *Macromol. Rapid Commun.* **2012**, *33*, 1286−1293.
(55) Seiffert, S.; Thiele, J.; Abate, A. R.; Weitz, D. A. Smart microgel capsules from macromolecular precursors. *J. Am. Chem. Soc.* **2010**, *132*, 6606−6609.
(56) Schild, H. G. Poly (N-isopropyacrylamide)-experiment, theory and application. *Prog. Polym. Sci.* **1992**, *17*, 163−249.
(57) Tanaka, T.; Fillmore, D. J. Kinetics of swelling of gels. *J. Chem. Phys.* **1979**, *70*, 1214−1218.
(58) Retama, J. R.; Lopez-Ruiz, B.; Lopez-Cabarcos, E. Micro-structural modifications induced by the entrapped glucose oxidase in cross-linked polyacrylamide microgels used as glucose sensors. *Biomaterials* **2003**, *24*, 2965−2973.
(59) Ge, H.; Ding, Y.; Ma, C.; Zhang, G. Temperature-controlled release of diols from N-isopropylacrylamide-co-acrylamidophenylboronic acid microgels. *J. Phys. Chem. B* **2006**, *110*, 20635−20639.
(60) Pich, A. Z.; Adler, H. J. P. Composite aqueous microgels: an overview of recent advances in synthesis, characterization and application. *Polym. Int.* **2006**, *56*, 291−307.
(61) Snedden, P.; Cooper, A. I.; Scott, K.; Winterton, N. Cross-linked polymer-ionic liquid composite materials. *Macromolecules* **2003**, *36*, 4549−4556.
(62) Xiong, Y.; Wang, H.; Wang, R.; Yan, Y.; Zheng, B.; Wang, Y. A facile one-step synthesis to cross-linked polymeric nanoparticles as highly active and selective catalysts for cycloaddition of CO2 to epoxides. *Chem. Commun.* **2010**, *46*, 3399−3401.
(63) Xiong, Y.; Wang, Y.; Wang, H.; Wang, R. A facile one-step synthesis to ionic liquid-based cross-linked polymeric nanoparticles and their application for CO_2 fixation. *Polym. Chem.* **2011**, *2*, 2306−2315.
(64) Xiong, Y.; Liu, J.; Wang, Y.; Wang, H.; Wang, R. One-step synthesis of thermosensitive nanogels based on highly cross-linked poly (ionic liquid) s. *Angew. Chem., Int. Ed.* **2012**, *51*, 9114−9118.
(65) Sahiner, N.; Yasar, A. The generation of desired functional groups on poly (4-vinyl pyridine) particles by post-modification technique for antimicrobial and environmental applications. *J. Colloid Interface Sci.* **2013**, *402*, 327−333.
(66) Schachschal, S.; Adler, H. J.; Pich, A.; Wetzel, S.; Matura, A.; van Pee, K. H. Encapsulation of enzymes in microgels by polymerization/cross-linking in aqueous droplets. *Colloid Polym. Sci.* **2011**, *289*, 693−698.
(67) Nur, H.; Pinkrah, V. T.; Mitchell, J. C.; Benee, L. S.; Snowden, M. J. Synthesis and properties of polyelectrolyte microgel particles. *Adv. Colloid Interface Sci.* **2010**, *158*, 15−20.
(68) Kim, K. S.; Vincent, B. pH and temperature-sensitive behaviors of poly(4-vinyl pyridine-co-N-isopropyl acrylamide) microgels. *Polym. J* **2005**, *37*, 565−570.
(69) Schmidt, M.; Nerger, D.; Burchard, W. Quasi-elastic light scattering from branched polymers: 1. Polyvinylacetate and polyvinylacetate—microgels prepared by emulsion polymerization. *Polymer* **1979**, *20*, 582−588.
(70) Senff, H.; Richtering, W. Temperature sensitive microgel suspensions: Colloidal phase behavior and rheology of soft spheres. *J. Chem. Phys.* **1999**, *111*, 1705.
(71) Chen, H.; Li, J.; Ding, Y.; Zhang, G.; Zhang, Q.; Wu, C. Folding and unfolding of individual PNIPAM-g-PEO copolymer chains in dilute aqueous solutions. *Macromolecules* **2005**, *38*, 4403−4408.
(72) Chen, H.; Zhang, Q.; Li, J.; Ding, Y.; Zhang, G.; Wu, C. Formation of mesoglobular phase of PNIPAM-g-PEO copolymer with a high PEO content in dilute solutions. *Macromolecules* **2005**, *38*, 8045−8050.
(73) Senff, H.; Richtering, W. Influence of cross-link density on rheological properties of temperature-sensitive microgel suspensions. *Colloid Polym. Sci.* **2000**, *278*, 830−840.
(74) Yuan, J.; Antonietti, M. Poly (ionic liquid) latexes prepared by dispersion polymerization of ionic liquid monomers. *Macromolecules* **2011**, *44*, 744−750.
(75) Fukae, K.; Terashima, T.; Sawamoto, M. Cation-condensed microgel-core star polymers as polycationic nanocapsules for molecular capture and release in water. *Macromolecules* **2012**, *45*, 3377−3386.
(76) Dash, S.; Murthy, P. N.; Nath, L.; Chowdhury, P. Kinetic modeling on drug release from controlled drug delivery systems. *Acta Pol. Pharm.* **2010**, *67*, 217−223.

(77) Algieri, C.; Drioli, E.; Donato, L. Development of mixed matrix membranes for controlled release of ibuprofen. *J. Appl. Polym. Sci.* **2013**, *128*, 754−760.